Energy Conversion and Management 304 (2024) 118208

Contents lists available at ScienceDirect

Energy Conversion and Management

journal homepage: www.elsevier.com/locate/enconman

Research paper

Quantifying the carbon footprint of energy storage applications with an energy system simulation framework — Energy System Network

Anupam Parlikar [a,*], Benedikt Tepe [a], Marc Möller [a], Holger Hesse [b], Andreas Jossen [a]

[a] Technical University of Munich (TUM), School of Engineering and Design, Department of Energy and Process Engineering, Chair of Electrical Energy Storage Technology (EES), Arcisstr. 21, 80333 Munich, Germany

[b] Kempten University of Applied Sciences, Faculty of Mechanical Engineering, Institute for Energy and Propulsion Technologies, Bahnhofstr. 61, 87435 Kempten, Germany

ARTICLE INFO

Keywords:
Energy system
Battery energy storage system
Energy System Network
Carbon footprint
Levelized Emissions of Energy Supply (LEES)
LEES
State of Carbon Intensity (SOCI)

ABSTRACT

Energy storage is a crucial flexibility measure to temporally decouple power generation from power demand and is touted as the missing link in realizing a decarbonized energy system based on renewable energy. Energy storage capacity buildup at all levels of the global energy system is expected to accelerate the decarbonization process. To this end, a coherent mathematical framework to ascertain the carbon footprint of localized energy systems with energy storage is indispensable. This article presents an open-source energy system simulation program — Energy System Network (ESN). A variety of energy system configurations can be simulated with the Python program, which incorporates key energy system components such as generation, grid, storage, and loads. ESN features an integrated bottom-up approach that combines energy system modeling with streamlined life cycle assessment techniques to quantify the carbon footprint of all components in a localized energy system. The lifecycle phases of each component, including production, operation, and end-of-life treatment, can be considered. Carbon footprint values are obtained for two demonstrative case studies with lithium-ion battery applications: energy arbitrage and home energy systems. The metric Levelized Emissions of Energy Supply (LEES) has been used to evaluate the carbon footprint of each application. An unconventional energy arbitrage strategy designed to exploit the grid carbon intensity spreads instead of the energy price spreads manages to achieve a LEES value about 17% lower than the conventional variant. The influence of rooftop solar generation, battery energy storage system, and the energy management strategy on the LEES values for a home energy system is explored. A maximum LEES reduction of over 37% vis-á-vis the base scenario was observed with optimal energy management for the solar generation and the battery system. The open-source availability of ESN can contribute to transparency, comparability, and reproducibility in carbon footprint assessments of localized energy systems with energy storage.

1. Introduction

The rapid expansion of renewable energy sources is a central feature of the transition toward a decarbonized energy landscape [1]. Energy system simulation models allow for analyzing system behavior and performance under different scenarios, considering factors such as energy sources, grid characteristics, system configurations, and energy management strategies. Energy system models are indispensable for understanding and analyzing complex energy systems. Through scenario analyses, policymakers, energy planners, and other stakeholders can obtain detailed insights into system behavior for optimal resource allocation [2]. A localized energy system comprises a combination of actors, which can be grouped into generation, storage, grid connection, and load components. These components operate in tandem to ensure energy supply and meet the specific needs of a particular application.

Energy storage is becoming increasingly crucial in integrating intermittent renewables, meeting peak electricity demand, and maintaining grid stability. Stationary lithium-ion BESSs are the leading technology due to their high energy density, efficiency, service life, and scalability [3,4]. With a favorable downward cost trend that further accentuates their attractiveness, the capacity buildup and deployment of these systems both continue to grow [5,6]. It is imperative to understand and quantify their environmental impact, particularly in terms of their carbon footprint. The carbon footprint of an energy storage system comprises the total greenhouse gas emissions associated with

* Corresponding author.
E-mail addresses: anupam.parlikar@tum.de (A. Parlikar), benedikt.tepe@tum.de (B. Tepe), marc.moeller@tum.de (M. Möller), holger.hesse@tum.de (H. Hesse), andreas.jossen@tum.de (A. Jossen).

https://doi.org/10.1016/j.enconman.2024.118208
Received 14 November 2023; Received in revised form 15 January 2024; Accepted 12 February 2024
Available online 20 February 2024

Abbreviations

BESS	Battery Energy Storage System
CO_2	Carbon Dioxide Equivalent
CO_2eq	Carbon Dioxide Equivalent
DEC	Discharge Energy Consumption
DOC	Depth of Cycle
EFC	Equivalent Full Cycle
EMS	Energy Management System
EOL	End-of-Life
ESN	Energy System Network
EV	Electric Vehicle
GEC	Grid Energy Consumption
GENEC	Generation Energy Consumption
GWP	Global Warming Potential
HES	Home Energy System
LCA	Life Cycle Assessment
LEC	Load Energy Consumption
LEES	Levelized Emissions of Energy Supply
PV	Photovoltaic Solar
SimSES	Simulation of Stationary Energy Storage Systems
SOC	State of Charge
SOCI	State of Carbon Intensity
SOH	State of Health

Parameters

CF^{gen}	Capacity Factor of generation component
$CI^{gen,exp,fix}$	Fixed component of the carbon intensity of the exported energy from a generation component
$CI^{gr,exp,fix}$	Fixed component of the carbon intensity of the exported energy with a grid component
$CI^{st,exp,fix}$	Fixed component of the carbon intensity of the exported energy discharged from a storage component
CI_t^{ch}	Carbon intensity of charging energy for BESS at time t
$CI_t^{st,exp}$	Carbon intensity of exported discharge energy from the storage at time t
$CI_t^{ES,exp}$	Carbon intensity of the export energy at time t
CI_t^{ES}	Carbon intensity of the energy at the central node of the energy system at time t
$CI_t^{gen,exp}$	Carbon intensity of the energy exported from the generation component at time t
CI_t^{gen}	Carbon intensity of the generation component at time t
$CI_t^{gr,exp}$	Carbon intensity of the energy exported with the grid component at time t
CI_t^{gr}	Effective carbon intensity of the grid mix at time t
$E^{s,EV}$	Energy supplied to the EV over the simulation period
$E^{s,H}$	Energy supplied to the household over the simulation period
$E_l^{st,dch}$	Total energy discharged by the storage technology over its service life
E_t^{st}	Energy content of the storage component at time t
$P^{gen,rated}$	Rated peak power of generation component
$P^{gr,peak}$	Peak power of the grid component
$P_t^{gen,can-run}$	Total power generation of all can-run generation components at the time t
$P_t^{gen,exp}$	Exported generation power from generation component at time t
$P_t^{gen,load,i}$	Directly consumed power generated by generation component i at the time t
$P_t^{gen,loss}$	Loss power of generation component at time t
$P_t^{gen,must-run}$	Total power generation of all must-run generation components at the time t
P_t^{gen}	Generation power of generation component at time t
$P_t^{gr,exp}$	Grid component export power at time t
$P_t^{gr,load}$	Grid power directly supplied to the load at time t
$P_t^{gr,loss}$	Power lost in the grid section during transmission at time t
P_t^{gr}	Total grid power entering the system boundaries at time t
$P_t^{load,c}$	Power consumed by end-application in a load component at time t
$P_t^{load,loss}$	Load loss power at time t
P_t^{load}	Load demand power at time t
$P_t^{residual}$	Residual power after factoring in total must-run generation power at the time t
$P_t^{st,ch}$	Storage component charging power at time t
$P_t^{st,dch,load,i}$	Directly consumed power discharged from storage component i at the time t
$P_t^{st,dch}$	Storage component discharging power at time t
$SOCI_t$	State of Carbon Intensity (SOCI) at time t
SOC_t	SOC at time t
Δt	Simulation timestep
η_t^{gen}	Generation component efficiency at time t
η_t^{gr}	Grid component energy efficiency at time t
$\eta_t^{st,ch}$	Storage component charging efficiency at time t
$\eta^{st,ch}$	Storage component average charging efficiency
$\eta_t^{st,dch}$	Storage component discharging efficiency at time t
$\overline{DOC}$	Mean DOC over simulation period
$\overline{SOCI}$	Mean SOCI over simulation period
$\overline{SOC}$	Mean SOC over simulation period
ε^{BESS}	Total emissions of the BESS over simulation period
ε^{DEC}	Total Discharge Energy Consumption (DEC) emissions for the load over simulation period
ε^{GENEC}	Total Generation Energy Consumption (GENEC) emissions for the load over simulation period

all its life cycle phases, which include production, operation, and end-of-life treatment. Calculating the carbon footprint requires accounting for numerous factors, including the energy mix used for charging the storage systems, energy losses during charge and discharge processes, storage degradation over time, and energy consumed for the production and recycling processes [7].

Estimating the carbon footprint is essential to informed decision-making in terms of the deployment of battery systems. A rigorous and

ε^{LEC}	Total Load Energy Consumption (LEC) emissions over simulation period
$\varepsilon^{gen,EOL}$	End-of-Life (EOL) phase emissions of the generation component
$\varepsilon^{gen,en}$	Total energy emissions for energy from on-site generation components
$\varepsilon^{gen,exp}$	Export emissions of the generation component
$\varepsilon^{gen,op}$	Operation phase emissions of the generation component
$\varepsilon^{gen,prod}$	Production phase emissions of the generation component
ε^{gr}	Total attributable emissions for the grid section over simulation period
$\varepsilon^{load,op}$	Operation phase emissions attributable to the load over the entire simulation period
ε^{load}	Total emissions attributable to the load over the entire simulation period
$\varepsilon^{st,EOL}$	EOL phase emissions of the storage component
$\varepsilon^{st,exp}$	Total export emissions of energy discharged from a storage component over simulation period
$\varepsilon^{st,op}$	Total operation phase emissions for the storage component
$\varepsilon^{st,prod}$	Production phase emissions of the storage component
ε^{st}	Total emissions of the storage component over simulation period
b_t^{st}	Binary variable to prevent simultaneous charging and discharging of the storage component at time t
c_t^{IDM}	Energy price on the Intraday Market at time t
h	Optimization time horizon h
m	Number of generation components in the energy system
n	Number of storage components in the energy system
p	Number of load components in the energy system
t	Time t
l^{gen}	Expected service lifetime of generation component in years

comprehensive analysis that captures the unique characteristics and application scenarios is indispensable. Various simulation models exist for modeling different aspects of the energy system with varying amounts of focus on battery systems, some of which have been published in open-source form. The following paragraphs briefly discuss the features of some existing energy system modeling tools.

Python for Power System Analysis (PyPSA) is an open-source toolbox developed in Python that provides functionalities for modeling, simulating, and optimizing power systems using power flow calculations and multi-period optimization. It is mainly used to create models of power networks, which include generators, power lines, and rudimentary storage systems. PyPSA can define and impose global constraints on Carbon Dioxide (CO_2) emissions during the optimization process. CO_2 emissions limits for different generation units can be specified by considering emissions factors associated with specific technologies [8]. EnergyPLAN is an open-source energy system modeling tool that facilitates the analysis and optimization of energy systems — from localized to national energy systems. Its main features include scenario analysis, renewable energy integration, energy system optimization, and multi-sectoral modeling. It also enables the specification of CO_2 emission factors for different energy generation technologies and sectors. The tool uses generic energy storage models. Carbon capture and storage can also be considered [9,10].

Calliope is an energy simulation Python tool designed to model and simulate national and urban scale energy systems designed to work with a variety of supply, transmission, storage, and demand technologies. The focus of performance evaluation is economic in nature. The program always solves an optimization problem to obtain the schedule for the energy system, and there is no possibility to run user-defined operation strategies. Time-resolved handling of the CO_2 emissions calculation for all components, especially for storage, is not supported [11,12]. Tools for Energy Model Optimization and Analysis (TEMOA) is another open-source modeling framework for performing energy system analyses and optimizations [13,14]. Temoa is a linear optimization problem that minimizes the costs of energy supply through the use of energy technologies and raw materials, such as coal or biomass, over defined time horizons. Quantification of C02 emissions from energy sources is also possible, albeit component-wise, and bottom-up time-resolved handling of the CO_2 emissions, especially for storage technologies, does not seem possible. The emissions can be limited via constraints of the linear optimization problem. TEMOA is an energy system optimization tool, i.e., it does not let users define their own energy management strategies [13,14].

urbs is a Python-based generator for linear energy system optimization models. The tool does not support user-defined energy management strategies, and the modeling capabilities for energy storage are elementary. The tool also does not support a very extensive CO_2 emissions calculation, especially for energy storage [15,16]. Oemof.solph is another open-source tool that can model and optimize energy systems as a Python package. In the optimization, a minimization of emissions can be defined as a constraint. According to the developers, the higher-level oemof (open energy modeling framework) can also minimize CO_2 emissions from biomass power plants [17,18]. The Framework for Integrated Energy System Assessment (FINE) is another Python-based open-source framework that enables the analysis and optimization of integrated energy systems. FINE can simulate energy systems ranging from localized to international. Entire electricity and natural gas grids can also be simulated. In addition, FINE models storage systems to a somewhat greater extent of detail than PyPSA and EnergyPLAN. Users can define CO_2 emission factors for different energy generation technologies, and in addition to economic optimization, they can also minimize CO_2 emissions [19,20].

GridLAB-D is a C++-based open-source power distribution system simulation and analysis tool that enables the simulation of electrical distribution networks, including storage and distributed energy resources. The tool does not provide built-in features dedicated to emissions modeling, although limited analyses to analyze certain scenarios are possible [21,22]. HOMER (Hybrid Optimization of Multiple Energy Resources) is a tool for analyzing and optimizing hybrid renewable energy systems. Its central capabilities include system optimization to determine cost-effective configurations, modeling renewable resources and loads, simulation and optimization of energy storage options, economic analysis, and the ability to conduct sensitivity analysis and explore different scenarios. Multiple commercial variants that deal with specialized aspects of energy system modeling are available: HOMER Pro, HOMER Grid, and HOMER Front. Homer Pro enables the calculation of CO_2 emissions based on specific emissions of the individual energy sources [23–25]. The System Advisor Model (SAM) is a tool that can be used to model renewable energy systems. SAM includes models for PV systems, storage systems of different types, and industrial processes. The models can be used directly in the desktop application and via application programming interfaces (APIs). CO_2 emissions can only be calculated in SAM in the Biomass Power model. Beyond that, no CO_2 calculations are carried out [26,27].

Distributed Energy Resource Value Estimation Tool (DER-VET^{TM}) is another option for the simulation and optimal design of microgrids,

storage systems, and distributed energy resources (DERs). The open-source tool is based on the StorageVET® tool, which can simulate storage systems in particular. CO_2 emissions are currently not modeled by DER-VET. However, integration of emissions modeling into the DER-VET optimization problem is planned, according to the developers [28]. Component-Oriented Modeling AND Optimization (COMANDO) is a framework for the design and operation of energy systems. Within COMANDO, an energy system is defined as a collection of different connected components. The tool solves optimization problems for the design and operation of energy systems. In contrast to other open-source tools, COMANDO does not rely solely on a linearization of the optimization problem but can also include dynamics and non-linear expressions. COMANDO does not allow user-defined energy management or customized energy system components. There is also no provision for a detailed CO_2 emissions calculation for components and for energy storage [29,30]. The Performance Simulation Model for Photovoltaic Solar (PV)-Battery Systems (PerMod), an open-source project, allows comparison of the energy efficiency of different grid-connected PV battery systems. This MATLAB-based tool can map different loss mechanisms of grid-connected PV storage systems. Accordingly, it enables a detailed simulation of households with home PV storage systems. Emissions modeling is not a part of the program [31].

A further Python-based optimization model for capacity expansion and unit commitment is ficus. This model focuses on determining the optimal size of system components, including energy storage, and their optimal operation scheduling. There is no provision to add user-defined operation strategies. The storage model used is generic. There is no known functionality to calculate the CO_2 emissions [32,33]. DRAF, short for Demand Response Analysis Framework, is an open-source tool for local multi-energy systems focusing on demand response, as the name suggests. DRAF is an optimization tool that employs linear and mixed-integer linear programming techniques. User-defined energy management strategies that rely on other optimization techniques or strategies that are rule-based cannot be implemented in DRAF. DRAF also includes elmada, a tool that can generate the grid carbon intensity profiles for European countries. The tool also relies on generic battery models which do not consider degradation. From the surveyed literature, the degree of detail in modeling the component-wise CO_2 emissions, especially for energy storage, could not be ascertained [34,35].

Two storage-centric simulation programs were also studied. The Battery Lifetime Analysis and Simulation Tool (BLAST) is a software tool specifically for analyzing and simulating battery systems. With BLAST, users can perform electrical and thermal simulations to assess the performance and lifetime of batteries. For example, BLAST-Lite is open-source and used in SAM to model storage systems. BLAST does not include a calculation of CO_2 emissions [36]. Simulation of Stationary Energy Storage Systems (SimSES) is a Python-based open-source tool that can simulate storage systems in various applications. SimSES does not offer emissions modeling capabilities. SimSES is used to model storage systems in ESN through a programmatic integration [37].

The reviewed energy system modeling tools are, for the most part, optimization tools that solve a particular form of sizing or scheduling problem. Applications and use cases that require very specific constraints and rules are difficult to simulate, thus restricting flexibility. The battery models employed in most tools are also generic in nature and not detailed enough. None of the tools reviewed offer specific capabilities to quantify and simulate the CO_2 emissions of energy storage systems operating in localized energy systems in a component-wise and time-resolved fashion. The specialized battery simulation tools, such as BLAST, SAM, and SimSES are well suited for modeling the electrical and thermal behavior of battery cells and storage systems but are limited in their ability to model the CO_2 emissions. These findings are corroborated by multiple review papers studying energy system models used in the scientific community [38–41]. Detailed tabular comparisons of the features of various energy system models were found in the reviewed literature, and the reader is referred to these excellent studies [34,38,39,41]. Studying the time-resolved carbon footprint of specific BESS applications in localized energy systems with detailed models is not possible with the reviewed energy system and energy storage models alone. This article presents Energy System Network (ESN),[1] a program to simulate localized energy systems with inherent bottom-up time-resolved capabilities to calculate the CO_2 emissions footprints of energy system components. ESN provides a platform to enable custom energy management strategies and specialized energy system components for any application as time series simulations. With seamless SimSES[2] integration allowing for detailed battery system modeling, ESN offers advanced simulation capabilities to simulate energy storage applications within localized energy systems. A reviewed study provides five modeling recommendations for the carbon footprint of energy storage systems [42]. ESN coupled with SimSES can aid users with four of the five recommendations pertaining to the inclusion of life cycle phases, energy management, and system components in such studies. The program is distributed as open-source code hosted on a Gitlab repository and is built with an object-oriented programming approach in Python.

Scope and outline

This article presents the simulation framework underpinning ESN, while attempting to shed light on the following research questions:

1. How can a coherent and unambiguous carbon emissions modeling framework for localized energy systems with energy storage be implemented such that the results are component-wise and time-resolved?
2. How can the carbon footprints of such localized energy system configurations providing a given service be compared consistently and reproducibly?

The use of this framework is demonstrated through case studies. An attempt is made to address the following research questions through the simulation of two battery storage system applications, energy arbitrage, and home energy systems:

1. Can the battery application energy arbitrage directly support grid decarbonization, and how can this be quantified?
2. How can the decarbonization impact of residential battery storage systems and rooftop solar generation in home energy systems be quantified?

The contents of this article are structured as follows. Section 2 presents the simulation framework behind ESN with the emissions modeling methods for all energy system component classes. The two case studies are presented in Section 3, accompanied by a discussion on the simulation setup and the simulation results. In Section 4, a summary of the current and possible future capabilities of ESN is presented along with the key findings and limitations of the case studies.

2. Simulation framework

This section presents the simulation framework behind ESN and the mathematical framework underpinning it. The simulation program is, in principle, designed to model multiple energy systems interacting with one another, i.e. an energy system comprised of multiple smaller energy systems. In its current state, ESN supports scenarios that can be modeled as a single energy system.

[1] https://gitlab.lrz.de/open-ees-ses/energy_system_network
[2] https://gitlab.lrz.de/open-ees-ses/simses

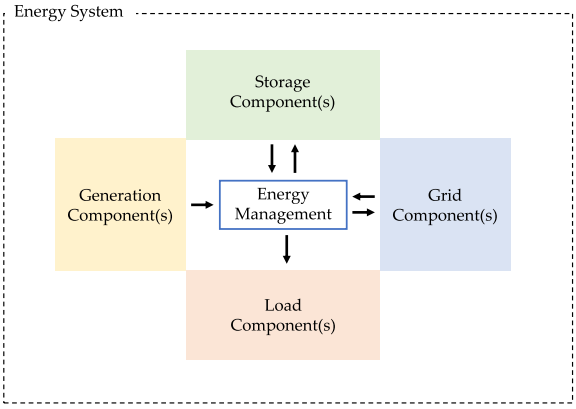

Fig. 1. Schematic representation of an *Energy System*, its constituent *Energy System Components*, and the Energy Management System (EMS) that regulates the power flows among them.

2.1. Energy system

An *Energy System* is a self-sufficient simulation unit representing a single node subjected to an energy balance. Each Energy System essentially represents a group of energy system components connected at the same node that directly satisfy the energy and power balance constraints at that node. Each energy system must consist of two or more *Energy System Components*, which belong to either of the four component classes:

1. Generation components
2. Grid components
3. Storage components
4. Load components

A grid component is a grid section that connects the node within the system boundaries to the larger energy system that lies beyond the boundaries. The operation and the energy flows among these components are regulated by algorithms in the Energy Management System (EMS), an instance of which is contained in each energy system. Fig. 1 depicts an energy system with its constituents.

The energy system components and their attributes are described in the following section. Models belonging to each component class emulate the central characteristics of each component class — generation, transmission, storage, or load. Each energy system component has a common structure: the physical model, time-series profiles, state, environmental data, and other additional component data. At the core of each component model lies the physical system of governing equations. This model enables the response of the component to be simulated. The components require user-defined or default profiles to model time-variant quantities such as generation, consumption, availability, and time-dependent carbon intensity. The environmental data pertains to its lifecycle emissions in all phases, including production, operation, power generation, and EOL processes. At each timestep, the EMS determines target powers for all components based on its algorithm. All quantities of interest are stored in the *State* of the EMS. Each energy system component receives the power target and runs it through the physical model to obtain the actual power. All parameters of interest are subsequently stored in the *State* of each component, which acts as a data logger. The contents of the state are analyzed and evaluated after each simulation run to obtain consolidated results for all components and the energy system.

The emissions calculation methodology for each component class is presented and discussed in the following sections. Documentation on installation, configuration, and exemplary simulations are found in the open-source code repository for the project. As this work focuses on the emissions modeling of localized energy systems, the following sections focus primarily on those aspects.

Table 1
Class attributes of energy system component classes.

	Energy system components			
	Generation	Grid	Storage	Load
Energy form applicable	x	x	x	x
Peak power	x	x	x	x
Energy capacity	–	–	x	–
State	x	x	x	x
Profile(s)	Generation	Carbon-Intensity	–	Load
Flag(s)	Must-run	Feed-in enabled		Must-fulfill
			–	Discrete load
Capacity factor	x	–	–	–
Production phase emissions	x	x	x	–
End-of-life emissions	x	x	x	–

2.2. Generation components

Generation components emulate the functioning of power generation systems. Each generation component exhibits class attributes tabulated in Table 1. Renewable energy sources such as PV solar and wind turbines are modeled using generation profiles for specified locations, whereas a diesel generator is modeled using an efficiency curve to model power output with respect to fuel consumption. For a generation component, the total emissions across its entire service life, ϵ^{gen}, are given by Eq. (1), where $\epsilon^{\text{gen,prod}}$, $\epsilon^{\text{gen,op}}$, and $\epsilon^{\text{gen,EOL}}$ refer to the production phase, operation phase, and EOL phase emissions respectively. Export emissions, $\epsilon^{\text{gen,exp}}$, are associated with the exported energy. This is discussed towards the end of this sub-section. Fig. 2 depicts the power flows and emissions associated with a generation component within the system boundaries.

$$\epsilon^{gen} = \epsilon^{gen,prod} + \epsilon^{gen,op} + \epsilon^{gen,EOL} - \epsilon^{gen,exp} \tag{1}$$

The total operation phase emissions, $\epsilon^{\text{gen,op}}$, can be calculated as shown in Eq. (2). Here, CI_t^{gen} refers to the carbon intensity of the generated energy before losses at time t and is equal to the combustion emissions per kWh of electricity for conventional generation components. For generation components such as the PV solar system and wind turbines, CI_t^{gen} is zero. $\text{P}_t^{\text{gen,loss}}$ is the loss power associated with an effective power generation P_t^{gen} at time t. P_t^{gen} does not include the exported power. Δt is the chosen simulation timestep. With this line of thought, the operation phase emissions for PV solar system and wind turbines are essentially zero.

$$\epsilon^{gen,op} = \sum_{t=start}^{end} (CI_t^{gen} \cdot P_t^{gen,loss}) \cdot \Delta t \tag{2}$$

The power generation emissions, $\epsilon^{\text{gen,en}}$, are allocated to all components either consuming or losing some of this generated energy during transmission or storage of this energy (Eq. (3)). For non-combusting generation components, $\epsilon^{\text{gen,en}}$ equals zero.

$$\epsilon^{gen,en} = \sum_{t=start}^{end} (CI_t^{gen} \cdot P_t^{gen}) \cdot \Delta t \tag{3}$$

The surplus energy produced by a generation component can also be exported to actors outside the system boundaries. The export emissions, $\epsilon^{\text{gen,exp}}$, are then obtained as follows (Eq. (4)), where $\text{P}_t^{\text{gen,exp}}$ is the exported generation power at time t. Here, $\text{CI}^{\text{gen,exp,fix}}$ refers to the fixed component of the emissions per unit of energy generated. These emissions are deducted from the total emissions of the generation component.

$$\epsilon^{gen,exp} = \sum_{t=start}^{end} \left(CI^{gen,exp,fix} \cdot P_t^{gen,exp}\right) \Delta t \tag{4}$$

$\text{CI}^{\text{gen,exp,fix}}$ is defined as in Eq. (5). CF^{gen} is the expected capacity factor for the generator at the specified location, $\text{P}^{\text{gen,rated}}$ is the rated

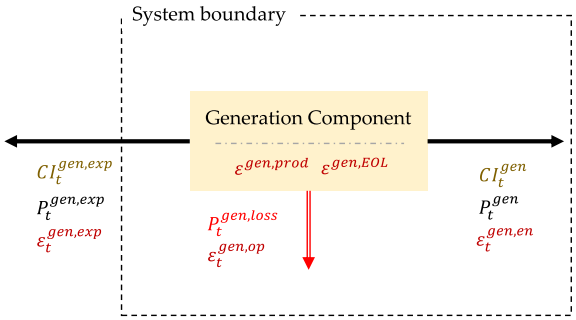

Fig. 2. Block diagram of a generation component depicting the power flows, emissions categories, and carbon intensities.

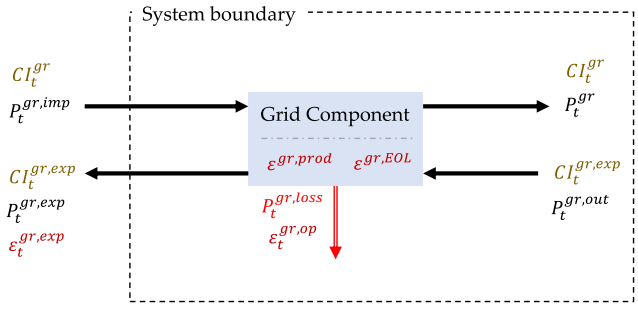

Fig. 3. Block diagram of a grid component depicting the power flows, emissions categories, and carbon intensities.

peak power, and l^{gen} is the expected service lifetime of the generation component.

$$CI^{gen,exp,fix} = \frac{\varepsilon^{gen,prod} + \varepsilon^{gen,EOL}}{CF^{gen} \cdot P^{gen,rated} \cdot l^{gen}} \tag{5}$$

The exported energy has a carbon intensity, $CI_t^{gen,exp}$, given by Eq. (6). The second term indicates the operation emissions associated with the generation of each unit of energy, where η_t^{gen} is the efficiency of the generation component at time t. These operation emissions are also reallocated to actors beyond the system boundaries. This second term is zero in the case of PV systems and wind turbines. Only the fixed component is considered.

$$CI_t^{gen,exp} = CI^{gen,exp,fix} + \frac{CI_t^{gen}}{\eta_t^{gen}} \tag{6}$$

ESN currently supports the calculation of export emissions for renewable generation components.

2.3. Grid components

Grid components emulate the functioning of grid connections or limited grid sections. Each grid component exhibits the attributes listed in Table 1. If the grid component is included in the system boundaries, the lifecycle emissions associated with it, ε^{gr}, are given by Eq. (7), where $\varepsilon^{gr,prod}$, $\varepsilon^{gr,op}$, and $\varepsilon^{gr,EOL}$, are the production, operation, and EOL phase emissions respectively. If a grid component is to be modeled purely as a grid connection, it is considered outside the system boundaries, with the connection itself enabling the import and export of power from the larger grid. In this case, no production and EOL emissions are associated with the grid component. If the grid component is excluded from the system boundary, ε^{gr} is merely equal to $\varepsilon^{gr,op}$. Export emissions, $\varepsilon^{gr,exp}$, are associated with the exported energy. This is discussed towards the end of this sub-section. Fig. 3 depicts the power flows and emissions associated with a grid component within and outside the system boundaries.

$$\varepsilon^{gr} = \varepsilon^{gr,prod} + \varepsilon^{gr,op} + \varepsilon^{gr,EOL} - \varepsilon^{gr,exp} \tag{7}$$

The total operation phase emissions, $\varepsilon^{gr,op}$, are calculated as follows, where CI_t^{gr} is the carbon intensity of the energy transported by the grid component. $P_t^{gr,loss}$ is the loss power associated with the effective imported grid power, P_t^{gr}, at time t.

$$\varepsilon^{gr,op} = \sum_{t=start}^{end} (CI_t^{gr} \cdot P_t^{gr,loss}) \cdot \Delta t \tag{8}$$

The grid energy import emissions, $\varepsilon^{gr,en}$, are allocated to all components either consuming or losing some of this imported energy during storage (Eq. (9)).

$$\varepsilon^{gr,en} = \sum_{t=start}^{end} (CI_t^{gr} \cdot P_t^{gr}) \cdot \Delta t \tag{9}$$

The export emissions to be deducted from the total emissions of the grid component are given by Eq. (10). $CI^{gr,exp,fix}$ is the fixed component of the export emissions, and $P_t^{gr,exp}$ represents the export power. A scheme to determine this fixed component, considering grid component production and EOL emissions, could also be devised, similar to the generation components. Given the high durability, correspondingly long service lifetimes, and ubiquitousness of grid components, this value is estimated to be negligible and is hence not considered further. Moreover, for grid components treated as mere grid connections, the value of $CI^{gr,exp,fix}$ would be zero, in any case, as the production and EOL phase emissions are also zero.

$$\varepsilon^{gr,exp} = \sum_{t=start}^{end} \left(CI^{gr,exp,fix} \cdot P_t^{gr,exp}\right) \Delta t \tag{10}$$

Depending on the sources of the exported energy, the carbon intensity of the exported energy, $CI_t^{ES,exp}$, is calculated below (Eq. (11)), where m is the number of generation components, and n is the number of storage components.

$$CI_t^{ES,exp} = \frac{\sum_{i=1}^{m} P_t^{gen,exp,i} \cdot CI_t^{gen,exp,i} + \sum_{j=1}^{n} P_t^{st,dch,exp,j} \cdot CI_t^{st,exp,j}}{\sum_{i=1}^{m} P_t^{gen,exp,i} + \sum_{j=1}^{n} P_t^{st,dch,exp,j}} \tag{11}$$

The carbon intensity of the exported energy through the grid component, $CI_t^{gr,exp}$, taking into account the additional emissions due to the operation losses in the grid section, is calculated as in Eq. (12), where η_t^{gr} is the efficiency of the grid component at time t.

$$CI_t^{gr,exp} = CI^{gr,exp,fix} + \frac{CI_t^{ES,exp}}{\eta_t^{gr}} \tag{12}$$

As it is cumbersome and infeasible to track the portion of exported energy first imported, Eq. (12) contains only a single efficiency term, corresponding to the losses in the export process, instead of two efficiency terms, as in the case of storage components. ESN does not currently support the calculation of export emissions for the grid components.

2.4. Storage components

Storage components model the characteristics of an energy storage system. The attributes of these components are listed in Table 1. The total emissions across the lifetime of a storage component, ε^{st}, consist of the production, operation, and EOL phases (Eq. (13)), represented by $\varepsilon^{st,prod}$, $\varepsilon^{st,op}$, and $\varepsilon^{st,EOL}$ respectively. If a portion of the discharged energy is exported outside the system boundaries, a corresponding amount of emissions $\varepsilon^{st,exp}$ is deducted from ε^{st}. This is discussed towards the end of this sub-section. Fig. 4 depicts the power flows and emissions associated with a storage component within the system boundaries.

$$\varepsilon^{st} = \varepsilon^{st,prod} + \varepsilon^{st,op} + \varepsilon^{st,EOL} - \varepsilon^{st,exp} \tag{13}$$

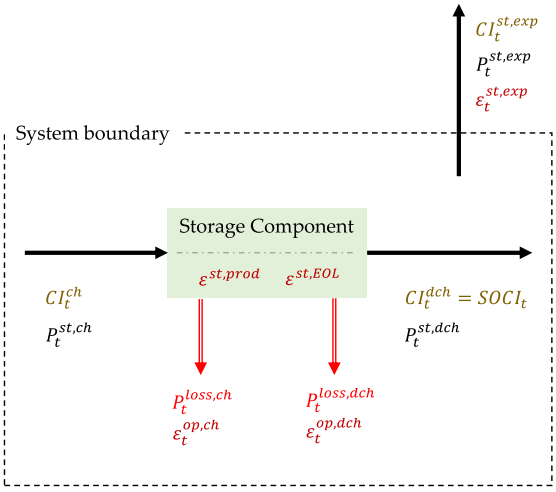

Fig. 4. Block diagram of a storage component, depicting the power flows, emissions categories, and carbon intensities.

The operations emissions of the charging process are proportional to the charging losses, $P_t^{ch,loss}$, of the storage component and the carbon intensity of the charging energy CI_t^{ch}. In the simplest case, CI_t^{ch} could be equal to the carbon intensity of the central energy system node CI_t^{ES} (Eq. (14)). In other cases, the storage might only be charged from energy sourced solely from one or more sources, in which case, CI_t^{ch} might need to be determined separately.

$$CI_t^{ES} = \frac{\sum_{i=1}^{m} P_t^{gen,i} \cdot CI_t^{gen,i} + CI_t^{gr} \cdot P_t^{gr}}{\sum_{i=1}^{m} P_t^{gen,i} + P_t^{gr}} \tag{14}$$

The operation phase emissions during discharge are proportional to discharge losses, $P_t^{dch,loss}$, and the SOCI, a new state variable, first introduced in a previous study [43]. The SOCI is defined as follows in Eq. (15), where $SOCI_t$ and SOC_t are the values of the SOCI and SOC variables at time t.

$$SOCI_{t+1} = \frac{SOCI_t \cdot SOC_t + \Delta SOC \cdot CI_t^{ch}}{SOC_{t+1}} \tag{15}$$

The total operation emissions $\varepsilon^{st,op}$ for the storage component consist of the operation emissions in the charging and the discharging processes. $\varepsilon^{st,op}$ is then obtained as the sum of emissions in the charging and discharging processes.

$$\varepsilon^{st,op} = \sum_{t=start}^{end} (CI_t^{ch} \cdot P_t^{ch,loss} + SOCI_t \cdot P_t^{dch,loss}) \cdot \Delta t \tag{16}$$

The export emissions to be deducted from the total emissions of the storage component are given by Eq. (17). The first term in the sum, $CI^{st,exp,fix}$, represents a reallocation of the fixed component of the storage component emissions, whereas the second term indicates the reallocation of the operation emissions associated with the charging and discharging of the exported energy. It is assumed that the discharged exported energy was charged with a carbon intensity equal to $SOCI_t$, with an efficiency equal to the average charging efficiency $\eta^{st,ch}$. $\eta_t^{st,dch}$ refers to the instantaneous discharging efficiency, and $P_t^{st,dch,exp}$ refers to the exported discharge power at time t.

$$\varepsilon^{st,exp} = \sum_{t=start}^{end} \left[\left(CI^{st,exp,fix} + SOCI_t \cdot \left(\frac{1}{\eta^{st,ch}\eta_t^{st,dch}} - 1 \right) \right) \cdot P_t^{st,dch,exp} \right] \Delta t \tag{17}$$

$CI^{st,exp,fix}$ is defined as in Eq. (18), where $E_l^{st,dch}$ is the total energy discharged by the storage technology over its service life. An estimate of this quantity can be obtained through prior simulations based on accurately parameterized battery degradation models or approximations

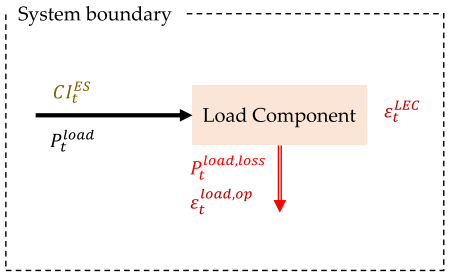

Fig. 5. Block diagram of a load component depicting the power flows, emissions categories, and carbon intensities.

based on values provided in datasheets. The carbon intensity of the exported energy, $CI_t^{st,exp}$, can then be simplified and written as follows (Eq. (19)).

$$CI^{st,exp,fix} = \frac{\varepsilon^{st,prod} + \varepsilon^{st,EOL}}{E_l^{st,dch}} \tag{18}$$

$$CI_t^{st,exp} = CI^{st,exp,fix} + \frac{SOCI_t}{\eta^{st,ch} \cdot \eta_t^{st,dch}} \tag{19}$$

ESN does not currently support the calculation of export emissions for the storage components.

2.5. Load components

Load components approximate the functioning of power consumers. Each load component exhibits the attributes listed in Table 1. The load power, P_t^{load}, supplied to the load can be divided into the actual power consumed by the end application, $P_t^{load,c}$, and the power lost to conversion processes, $P_t^{load,loss}$, for example in the charger of an EV (eq, (20)) (see Fig. 5).

$$P_t^{load} = P_t^{load,c} + P_t^{load,loss} \tag{20}$$

Over the simulated period, the total emissions allocated to a load component, ε^{load}, are given by Eq. (21), where ε^{LEC} are the Load Energy Consumption (LEC) emissions, and $\varepsilon^{load,op}$ are the operation emissions assigned to the load (if required). The carbon intensity of the energy at the central node, CI_t^{ES}, is calculated as in Eq. (14). The total operation phase emissions of the load component are calculated as the sum of the products of the load loss power $P_t^{load,loss}$ and the carbon intensity of the energy consumed by the load, CI_t^{ES} (Eq. (23)).

$$\varepsilon^{load} = \varepsilon^{LEC} + \varepsilon^{load,op} = \sum_{t=start}^{end} (P_t^{load} \cdot CI_t^{ES}) \cdot \Delta t \tag{21}$$

$$\varepsilon^{LEC} = \sum_{t=start}^{end} (P_t^{load,c} \cdot CI_t^{ES}) \cdot \Delta t \tag{22}$$

$$\varepsilon^{load,op} = \sum_{t=start}^{end} (P_t^{load,loss} \cdot CI_t^{ES}) \cdot \Delta t \tag{23}$$

The LEC emissions, ε^{LEC}, are obtained as a sum of the GENEC, the Grid Energy Consumption (GEC), and the DEC emissions (Eq. (24)). The Generation Energy Consumption (GENEC) emissions, ε^{GENEC}, are the sum of emissions on account of direct consumption of energy produced by the generators (Eq. (25)). The Grid Energy Consumption (GEC) emissions, ε^{GEC}, are the sum of emissions on account of direct consumption of energy imported from the grid (Eq. (26)). The Discharge Energy Consumption (DEC) emissions, ε^{DEC} are the sum of emissions on account of direct consumption of energy discharged from the storage components (Eq. (27)). $P_t^{gen,load,i}$ refers to the direct

consumption of power from generation component i at time t. $P_t^{gr,load}$ represents the direct consumption of grid power at time t. Similarly, $P_t^{st,dch,load,i}$ signifies the direct consumption of power discharged by storage component i at time t. By definition, the GENEC emissions for power generated by PV solar systems and wind turbines are zero.

$$\varepsilon^{LEC} = \varepsilon^{GENEC} + \varepsilon^{GEC} + \varepsilon^{DEC} \tag{24}$$

$$\varepsilon^{GENEC} = \sum_{t=start}^{end} \sum_{i=1}^{m} (CI_t^{gen,i} \cdot P_t^{gen,load,i}) \cdot \Delta t \tag{25}$$

$$\varepsilon^{GEC} = \sum_{t=start}^{end} (CI_t^{gr} \cdot P_t^{gr,load}) \cdot \Delta t \tag{26}$$

$$\varepsilon^{DEC} = \sum_{t=start}^{end} \sum_{j=1}^{n} (SOCI_t^{j} \cdot P_t^{st,dch,load,j}) \cdot \Delta t \tag{27}$$

2.6. Emissions balance and general discussion

With the quantities introduced and defined in the previous sections, an emissions balance for the energy system within the specified system boundaries can be obtained. This balance excludes the exported energy and only considers the actual energy quantities consumed or lost within the system boundaries (Eq. (28)), where p is the number of load components in the energy system.

$$P_t^{gr,imp} \cdot CI_t^{gr} + \sum_{i=1}^{m} \frac{P_t^{gen,i}}{\eta_t^{gen,i}} CI_t^{gen,i} = \varepsilon_t^{gr,op} + \sum_{i=1}^{m} \varepsilon_t^{gen,op,i} + \sum_{j=1}^{n} \varepsilon_t^{st,op,j} + \sum_{k=1}^{p} (\varepsilon_t^{LEC,k} + \varepsilon_t^{load,op,k}) \tag{28}$$

From the presented mathematical framework, from an allocation perspective, emissions during the operation phase can:

1. originate within the system boundaries (e.g., from a combustion-based generator)
2. enter the system boundaries from a source beyond the system boundaries (e.g., through a grid connection)
3. terminate at one or more components within the system boundaries (e.g., operation and energy consumption emissions)
4. exit the system boundaries and terminate at components outside the system boundaries (via exported energy)

Production phase and EOL phase emissions of all components within the system boundaries are allocated to the energy system. Some emissions are deducted from each component due to the exported energy. The choice of system boundaries depends on the purpose of a simulation. If the sole purpose of a simulation is to compare two competing system configurations, all common fixed elements may be disregarded, as these merely introduce a fixed offset in both analyses. In this case, the LEES values of the two competing configurations do not reflect absolute values but help determine the delta in this case. If some energy system components have a service lifetime longer than the simulated duration and are expected to still possess a so-called Remaining Useful Life (RUL), specific adjustments can be made to deduct a suitably determined quantity of emissions. The same applies to components that need to be replaced during the simulated duration and do not reach their EOL by the end of the simulated period. Table 2 lists the emissions categories applicable to each class of energy system components.

Table 2
Emissions categories applicable to each energy system component class.

		Emissions categories			
		Generation	Grid	Storage	Load
Static	Production	x	x	x	–
	End-of-life	x	x	x	–
Time-dependent	Operation	x	x	x	–
	Export	x	x	x	–
	Generation energy consumption	–	–	–	x
	Grid energy consumption	–	–	–	x
	Discharge energy consumption	–	–	–	x

2.7. Energy management

Each energy system possesses an Energy Management System (EMS). The EMS regulates the energy flows among the various components in an energy system by generating reference powers for all components while considering the specified constraints. Each EMS consists of two blocks: an operation strategy, which defines the logic/algorithm to govern energy flows, and a *State*, where values of all parameters are logged at each time t. The state enables subsequent analyses to be conducted after each simulation run. Two types of strategies regulate the energy flows with the EMS: rule-based and optimization-based strategies. The modular nature of ESN allows for the incorporation of new tailor-made rule-based and optimization-based strategies to suit the specific requirement of the user and the use case to be simulated.

2.7.1. Rule-based strategies

Rule-based strategies regulate the energy flows among components of the energy system based on a set of sequential commands or rules that depend on certain conditions being met. Three available rule-based strategies in ESN are discussed in the following sub-sections.

SimpleDeficitCoverage. The EMS strategy *SimpleDeficitCoverage* relies on a specified priority list of energy system components to meet the load power demand. The power generation of the must-run generation components (generation from PV solar and wind is also classified as such in many jurisdictions) is factored in first at every timestep (Eq. (29)). $P_t^{residual}$ refers to the residual power after factoring in the must-run generation, whereas $P_t^{gen,must-run}$ refers to the total generation power of all must-run generation components. Users can then specify which energy system component is to be used first, second, or third to meet the residual demand. The default priority list is as follows:

(I) Storage components
(II) Grid components
(III) Can-run generation components

With the default specification, the strategy attempts to meet the residual load first with discharged energy from the storage components. If available, the power is drawn from the grid components next. If further power is required, can-run generation components (such as the diesel generator) are run to deliver the demanded power (Eq. (30)). Here $P_t^{gen,can-run}$ refers to the total can-run generation power requested.

$$P_t^{residual} = P_t^{load} - P_t^{gen,must-run} \tag{29}$$

$$(P_t^{st,dch})^{I} + (P_t^{gr})^{II} + (P_t^{gen,can-run})^{III} = P_t^{residual} \tag{30}$$

The same priority is used to regulate the order of absorption of surplus generation from the must-run generation components. In the default setting, surplus generation is used to charge the storage components before being fed back into the grid. This strategy has been successfully demonstrated to control the energy system components operating in an island grid [44].

SimplePeakShaving. The EMS strategy *SimplePeakShaving* controls power flows in energy systems with constrained grid connections. Peak shaving is performed with a storage component that discharges additional power in parallel to meet the peak power demand. Must-run generation components can also be included. If the load power exceeds the rated power rating of the grid connection (and possibly

power generated by the must-run components), the residual load is met by discharging energy from the storage component. The storage component is recharged at maximum available power as soon as the load power goes below the rated grid power, and grid capacity is available to recharge the storage component (Eq. (31)).

$$P_t^{residual} = P_t^{load} - P_t^{gr} \tag{31}$$

This strategy has been successfully demonstrated in the provision of peak shaving service for EV high-power charging stations [43].

SimSESExternalStrategy. The EMS strategy *SimSESExternalStrategy* is used to operate the BESS based on power targets directly generated by EMS strategies available in SimSES. This EMS strategy currently supports the SimSES strategy *FcrIdmRechargeStacked*, which has been presented in a previous publication [37]. This strategy generates power targets for the BESS that react to the frequency fluctuations, allowing participation in the grid frequency regulation market. Further information on this strategy can be found in the SimSES project git repository.

2.7.2. Optimization-based strategies

Optimization-based strategies rely on mathematical optimization, rather than a set of rules, to determine the power targets for all energy system components. A suitably chosen objective function governs the optimum power values at each timestep. All optimization-based strategies in ESN currently rely on linear and mixed integer linear optimization to obtain the optimal energy flows. Two such strategies are discussed in the following subsections.

RHOptimization. The strategy *RHOptimization* regulates energy flows by solving a Rolling Horizon (RH) optimization problem to generate power targets for all components. The users can set the time span of the optimization horizon (h) and the frequency of re-optimization based on their requirements. This is a general-purpose strategy designed to handle multiple components with the sole aim of meeting load demand with the available energy system components while minimizing the emissions over each optimization horizon. The objective function deployed in this strategy attempts to minimize the emissions in each optimization horizon (Eq. (32)).

$$\min \sum_{t=t}^{t+h} \left[P_t^{gr} \cdot CI_t^{gr} + \sum_{i=1}^{m} (P_t^{gen,i} \cdot CI_t^{gen,i}) \right] \tag{32}$$

The following peak power constraint applies to each generation and grid component in the energy system to formulate the optimization problem. $P_t^{gen,peak}$ and $P^{gr,peak}$ refer to the peak power generation capability of the generation component and the peak power capability of the grid component, respectively, at time t (Eq. (33),(34)).

$$P_t^{gen} \le P_t^{gen,peak} \tag{33}$$

$$P_t^{gr} \le P^{gr,peak} \tag{34}$$

The following set of constraints applies to each storage component in the energy system and during the optimization problem formulation. Where $P_t^{st,ch}$ and $P_t^{st,dch}$ refer to the charging and discharging powers, respectively, of the storage component at time t. $P^{st,peak}$ refers to the storage peak power, while b_t^{st} represents the binary variable used to prevent simultaneous charging and discharging of the storage component at time t. $\eta_t^{st,ch}$ refers to the charging efficiency of the storage component at time t. E_t^{st} represents the energy content of the storage component at time t.

$$P_t^{st,ch} - b_t^{st} \cdot P_{peak}^{st} \le 0 \tag{35}$$

$$P_t^{st,dch} + (b_t^{st} - 1) \cdot P_{peak}^{st} \le 0 \tag{36}$$

$$0 \le SOC_t \le 1 \tag{37}$$

$$SOC_{t-1} \cdot E_t^{st} + (P_t^{st,ch} \cdot \eta_t^{st,ch} - \frac{P_t^{st,dch}}{\eta_t^{st,dch}}) \cdot \Delta t = SOC_t \cdot E_t^{st} \tag{38}$$

$$P_t^{st,ch} \cdot \eta_t^{st,ch} \cdot \Delta t \le \left(1 - SOC_{t-1}\right) \cdot E_t^{st} \tag{39}$$

$$\frac{P_t^{st,dch}}{\eta_t^{st,dch}} \cdot \Delta t \le SOC_{t-1} \cdot E_t^{st} \tag{40}$$

The following energy balance constraint applies to the energy system, ensuring that the sum of all component powers and allocations equals zero (Eq. (41)).

$$P_t^{gr} + \sum P_t^{st,dch} + \sum P_t^{gen} = P_t^{load} + \sum P_t^{st,ch} \tag{41}$$

A previous study successfully demonstrated this strategy on battery-assisted high-power charging for EVs [43].

ArbitrageOptimization. The *ArbitrageOptimization* strategy determines the scheduling of a grid-connected storage component such as BESS participating in energy arbitrage to buy and sell power on the intraday market. The strategy has been designed to optimize one of two objective functions — one that maximizes monetary profit and another that maximizes the difference between the product of grid carbon intensity and storage power during charging and discharging. The second objective essentially directs the storage to charge at low grid carbon intensity values and discharge at times of high grid carbon intensity values. The objective functions used in the economic and emissions-drive optimization are given in Eqs. (42) and (43) respectively. c_t^{IDM} represents the energy price on the intraday market at time t.

$$\max \sum_{t=t}^{t+h} \left[(P_t^{st,ch} + P_t^{st,dch}) \cdot c_t^{IDM} \right] \cdot \Delta t \tag{42}$$

$$\max \sum_{t=t}^{t+h} \left[(P_t^{st,ch} + P_t^{st,dch}) \cdot CI_t^{gr} \right] \cdot \Delta t \tag{43}$$

The storage component constraints (Eq. (35) to (40)) described under RHOptimization are also applicable to the optimization problem in this strategy. Further documentation and simulation examples can be found on the project git repository.

3. Case studies with typical applications

Simulation results of selected case studies to demonstrate the quantification of the total emissions over the lifecycle of an energy system are presented and discussed in this section. As the leading energy storage technology, we focus on lithium-ion Battery Energy Storage System (BESS) technology. In Section 3.1, a typical grid-connected application for BESSs is simulated — Energy Arbitrage. In Section 3.2, four typical Home Energy System (HES) scenarios with electromobility, rooftop solar, and home storage systems are simulated and discussed from the emissions perspective. In addition to the case studies presented here, this framework has already been successfully applied to applications such as island grids and EV high-power charging [43,44].

3.1. Energy arbitrage

Several energy markets exist to ensure a balanced grid at all times. BESSs can participate in these markets and provide services conveniently owing to their attributes. In these applications, the BESS interacts solely with the grid, charging and discharging energy from and to the grid. Typical system boundaries, power flows, and emissions categories are depicted in Fig. 6A. As the BESS is charged solely with power imported from the grid, the carbon intensity of the charging energy (CI_t^{ch}) is equal to the carbon intensity of power imported from the grid (CI_t^{gr}). The total emissions of the BESS across all phases is given by ε^{BESS}.

$$\varepsilon^{BESS} = \varepsilon^{BESS,prod} + \varepsilon^{BESS,op} + \varepsilon^{BESS,EOL} \tag{44}$$

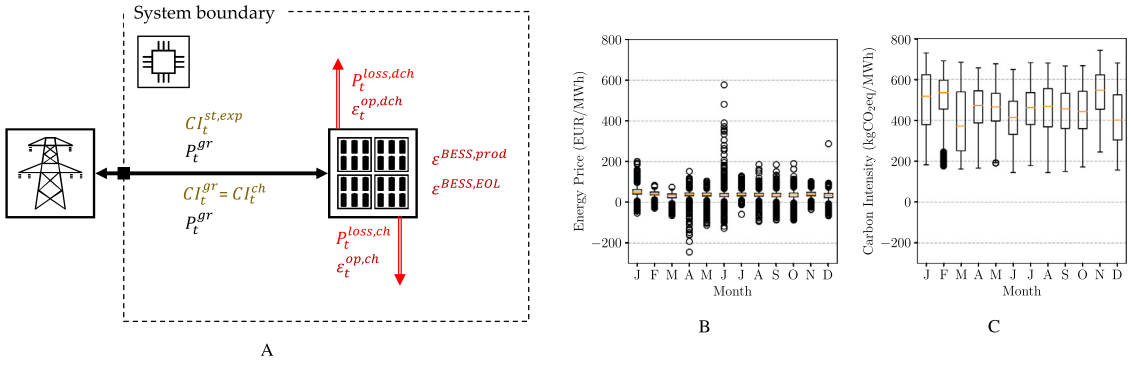

Fig. 6. C: Power flows and emissions categories for a typical grid-connected storage application. B: Depiction of the monthly energy price spreads on the Intraday Market over one year. C: Monthly variation in the Grid carbon intensity (CI_t^{gr}) over the selected year. Data for Germany for the year 2019.

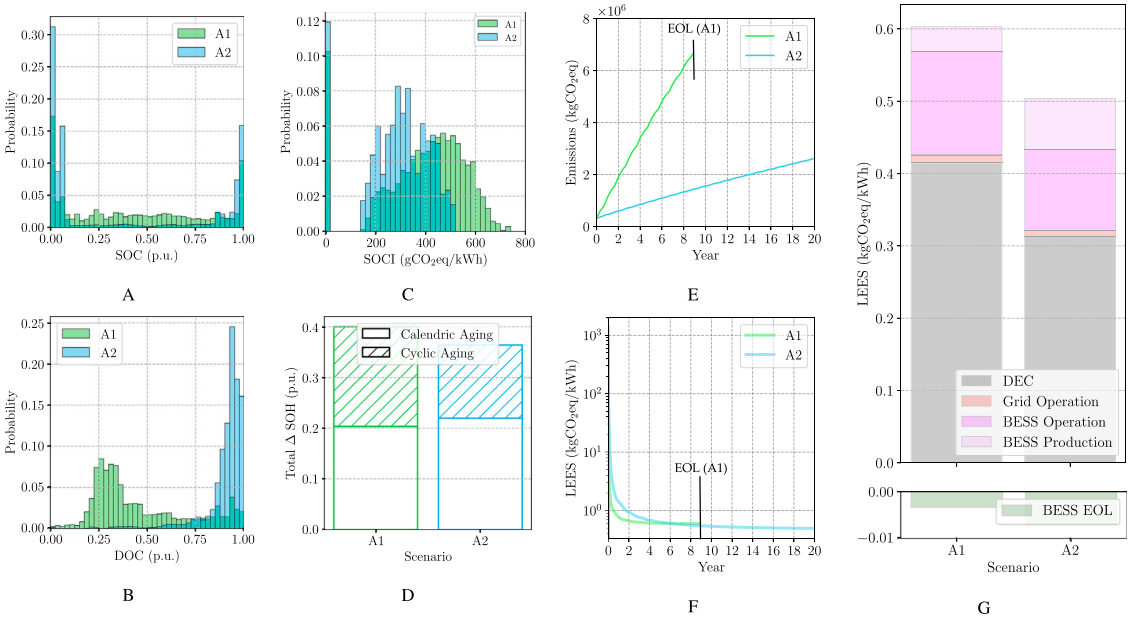

Fig. 7. A, B: Distributions of SOC and DOC values respectively in scenarios A1 and A2 over the simulated period. C: Distribution of the State of Carbon Intensity (SOCI) values in scenarios A1 and A2 over the simulated period. D: Change in the battery SOH over the simulated period and shares of calendric and cyclic aging in scenarios A1 and A2. E: Cumulative emissions for the two scenarios over the simulated period. F: Evolution of the Levelized Emissions of Energy Supply (LEES) value for the two scenarios over the simulated period. G: Breakdown of LEES values for the two scenarios into the constituent emissions categories at the end of the simulation period.

As a simplification, the grid can be considered a load, which consumes energy discharged by the BESS. The LEC emissions for this hypothetical load are solely made up of the DEC emissions (Eq. (45)). Levelized Emissions of Energy Supply (LEES) is a useful metric to obtain the carbon footprint of the energy supplied to a load [44]. The LEES value for the application enables us to look at the BESS as a grid-connected generator with a carbon intensity equal to LEES. This is akin to a retrospective calculation of the carbon intensity of the exported energy $CI_t^{st,exp}$ for the BESS (Eq. (46)).

$$\varepsilon^{DEC} = \sum_{t=start}^{end} SOCI_t \cdot P_t^{st,dch} \cdot \Delta t \tag{45}$$

$$LEES = \frac{\varepsilon^{BESS} + \varepsilon^{DEC}}{E^{dch}} \tag{46}$$

The price spreads on various energy markets, such as the Intraday and Day-Ahead markets, present energy arbitrage opportunities. Figs. 6B,C depict the spreads in the average 15-minute prices on the Intraday-Continuous (IDC) market and the spreads in the grid carbon intensity for the year 2019 in Germany. The price profile used has been generated from data obtained from the *energy-charts*[3] project [45]. The grid carbon intensity profile is also based on data from the same database combined with other data [43]. A conventional energy arbitrage scenario (A1) to maximize economic profit is simulated in this section alongside a novel emissions-arbitrage scenario (A2). The scenarios demonstrate the effect of the EMS strategy on the LEES values of the arbitrage application. The *ArbitrageOptimization* EMS strategy presented earlier (Section 2.7) is used in this application. An identical BESS system configuration is deployed in both scenarios to enable a fair comparison (see Table 3). Table 4 presents the streamlined LCA for the BESS system.

In scenario A1, the EMS strategy is set to generate the economically optimal BESS dispatch schedule. The SOC values are spread across the entire range from 0 to 1, with peaks around both 0 and 1 (depicted in Fig. 7A). As the spread in prices is relatively narrow, with a significant number of outliers, the BESS operates with a lot of shallow half-cycles with a DOC peak around 0.25 (depicted in Fig. 7B). Since the strategy responds to the spread in the energy prices, the distribution of the SOCI

[3] https://energy-charts.info/

Table 3
Battery Energy Storage System (BESS) configuration for participating in energy arbitrage.

Energy arbitrage	
Parameter	Value
Cell type	Lithium Iron Phosphate (LFP)
Cell format	Cylindrical, 26650
Rated energy capacity (MWh)	1.6
Rated power (MW)	1.6
Initial State of Health (SOH)	100%
Battery model	R-int Equivalent Circuit Model (ECM) (based on [46,47])
Battery degradation model	Semi-empirical calendric and cyclic (based on [48,49])
Power electronics	AC/DC Converter, 8 units (based on [50–52])
Housing type	40 ft. standard shipping container
HVAC thermal power (kW)	50
Ambient conditions	Berlin
Grid section efficiency	95% (assumed)

Table 4
Streamlined LCA for a utility-scale grid-connected Battery Energy Storage System (BESS) (based on [44]).

Battery Energy Storage System (BESS) streamlined LCA			
Component	Production ($kgCO_2eq$)	End-of-Life (EOL) ($kgCO_2eq$)	Source
Cells	257592.79	−18719.48	[53,54]
Power Electronics	61535.83	−15124.78	[55–58]
Miscellaneous Electronics	25235.73	−3656.66	[55,58]
Housing	28810.92	0.00	[55]
HVAC	426.12	0.00	[59]
Sum	373601.39	−37500.91	
Total	**336100.48**		

Table 5
Simulation results for the two energy arbitrage scenarios.

Simulation results energy arbitrage			
	Scenario		
Parameter	A1	A2	Δ%
Application			
Energy bought (GWh)	14.91	7.11	−52.29
Energy sold (GWh)	11.11	5.29	−52.35
Energy costs (k€)	383.94	172.43	−55.09
Revenue (k€)	548.75	293.51	−46.51
Profit (k€)	164.81	121.08	−26.53
Cumulative emissions (tCO_2)	6664.47	2630.39	−60.53
System temporal utilization (%)	86.00	31.00	−63.95
Fulfillment ratio (%)	87.86	99.60	13.36
LEES ($kgCO_2eq/kWh$)	0.5997	0.4968	−17.15
BESS			
Lifetime (y)	9	20	122.22
Round-Trip Efficiency (%)	74.53	74.43	−0.13
Remaining Capacity (%)	60	63.6	6.00
$\overline{SOC}$ (%)	43.51	37.67	−13.42
$\overline{DOC}$ (%)	46.43	90.44	94.79
Equivalent Full Cycles (EFCs)	8506.6	4063	−52.24
Mean C-rate (ch) (1/h)	0.79	0.75	−5.06
Mean C-rate (dch) (1/h)	0.84	0.77	−8.33
$\overline{SOCI}$ (gCO_2eq/kWh)	388.27	284.73	−26.67

values (Fig. 7C) are observed to tend towards the distribution of the grid carbon intensity (Fig. 8A) without any preference. The BESS is subjected to over 8500 EFCs in this application, and the EOL criterion (SOH = 0.6) is reached in around nine years of operation. The BESS

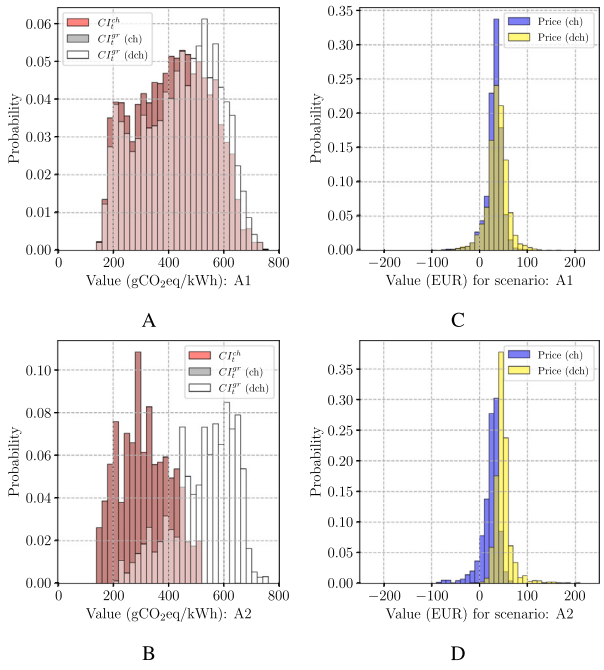

Fig. 8. A, B: Depictions of distributions of CI_t^{ch}, CI_t^{gr} during charging and CI_t^{gr} during discharging in scenarios A1 and A2, respectively. C and D: Distributions of energy price values during charging and discharging in scenarios A1 and A2, respectively.

loses 40% of its initial energy storage capacity within the operation period, with over 49% of this capacity loss occurring due to cyclic degradation mechanisms (Fig. 7D). Fig. 8A depicts the grid carbon intensity, CI_t^{gr} during charging and discharging. As the strategy does not take CI_t^{gr} into account, no pattern is discernible in the two distributions during charging and discharging can be observed. Fig. 8C depicts the energy prices during charging and discharging. It can be seen that the EMS strategy charges and discharges the BESS at a wide range of prices. A round-trip efficiency value of 77% is considered in the optimization algorithm. Corresponding to this value, a minimum price difference of around 29% between the buy and sell prices is required for the BESS to enter into energy arbitrage.

In scenario A2, the EMS strategy is set to determine the optimal BESS dispatch schedule to shift energy from periods of low CI_t^{gr} to periods of high CI_t^{gr}. A BESS operating in this mode can essentially be considered as supporting the firming of renewable energy generation. The SOC values are skewed much stronger to the extremes with a sparser distribution over the intervening values (Fig. 7A). The BESS is cycled much less (over 4063 EFCs), albeit with higher DOC values (Fig. 7B). The distribution of the SOCI values is shifted leftwards, as the BESS specifically charges when CI_t^{gr} is low (Fig. 7C). The BESS is cycled gentler and reaches an SOH value of around 63% at the end of 20 years. The contribution of cyclic degradation to this capacity loss is over 39% (Fig. 7D). Fig. 8B depicts the distributions of the values of CI_t^{gr} during charging and discharging. A clear separation in the two distributions can be seen, with a preference to charge when CI_t^{gr} assumes relatively lower values and discharging at times that coincide with higher CI_t^{gr} values. A distinct separation in the distributions of the energy prices during charging and discharging can also be observed here (Fig. 8D). This can be explained by the observation that the energy prices positively correlate to the grid carbon intensity values with a correlation coefficient of 0.6132 for 2019. With a round-trip efficiency of around 77%, a minimum ΔCI_t^{gr} of around 29% is required for the BESS to enter into the energy arbitrage.

In Fig. 7E, the cumulative emissions in scenarios A1 and A2 are depicted. As the energy throughput in scenario A1 is higher than in scenario A2, the variable emissions categories (DEC emissions, BESS

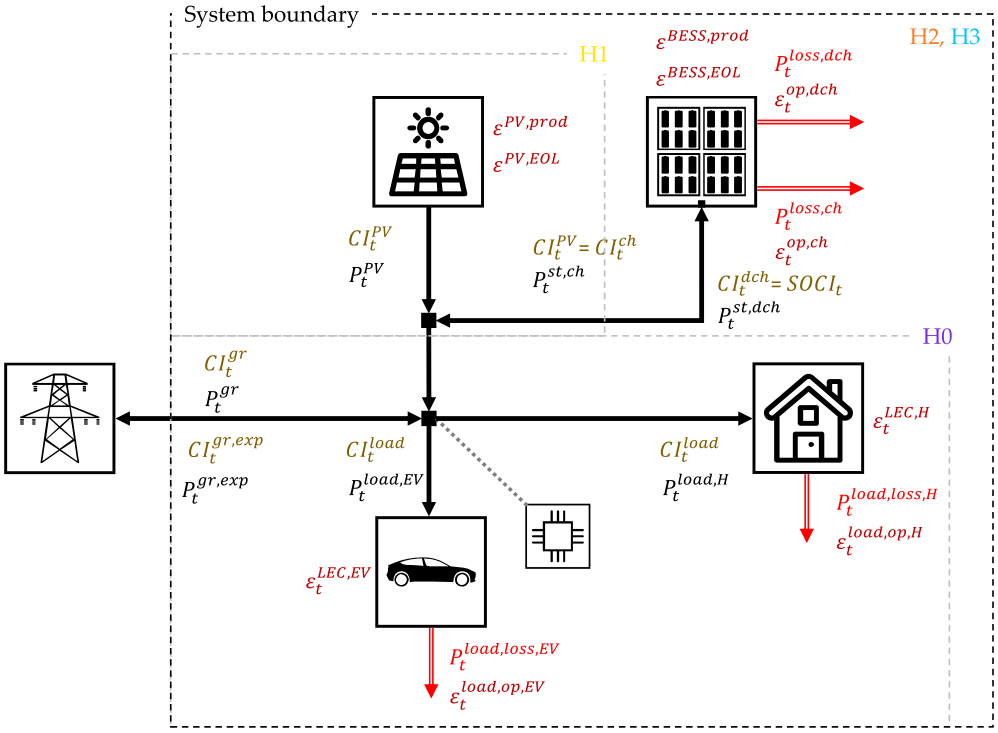

Fig. 9. Power flows and emissions categories for a typical Home Energy System (HES). The four scenarios H0, H1, H2, H3 are depicted here.

operation emissions, and the grid operation emissions) rise faster than in scenario A2. Fig. 7F depicts the evolution of the LEES values over the simulated period. Although a lower LEES value is exhibited in scenario A1 in the first five years, due to the higher energy throughput, from the fifth year onward, scenario A2 exhibits a consistently lower LEES value until the end of the simulation period. Fig. 7G depicts a snapshot of the emissions category-wise breakdown of the LEES value at the end of the simulated period in each scenario. Scenario A1 has a LEES value of 0.5997 $kgCO_2/kWh$, whereas A2 exhibits a LEES value of 0.4968 $kgCO_2/kWh$, which is over 17% lower than that of scenario A1. This trend is also supported by the movement in the mean SOCI values, which in scenario A2 is over 26% lower than in A1. Table 5 summarizes the salient numerical results of each scenario. Despite 52% lower volumes of energy sold, the profit in scenario A2 is only about 26% lower, whereas the cumulative emissions are over 60% lower. Figs. A.1 A,D in the appendix depict the grid carbon intensity and the energy prices during exemplary winter and summer weeks, respectively. Figs. A.1 and A.2 in the appendix also depict the evolution of other parameters of interest.

3.2. Home Energy System (HES)

HESs are gaining in popularity as the prices of PV installations and residential BESSs continue on their downward trend [63]. An additional factor underpinning the popularity of such systems is the rise of electromobility and potential synergies. Studies in the reviewed literature present some form of rules-based emissions-aware EMS strategies to operate a PV-coupled BESS to increase the emissions saving [64]. This section illustrates the modeling and simulation of four HES scenarios (H0, H1, H2, H3) to obtain their Global Warming Potential (GWP) footprints over an operation period of 20 years. A grid-connected household with an EV is considered in this case study (Fig. 9). The annual household load profile is based on a standard profile published by the authors in a previous work [65]. This standard profile is based on a published collection of 74 household load profiles [66]. The profile has an annual household energy consumption of around 4360 kWh. The EV charging load profile is based on simulated data for a Volkswagen ID.3, which is generated with data obtained from the *emobpy* tool and simulated separately with SimSES. This profile has an annual energy consumption of over 1927 kWh [67]. In general, the LEES values for these scenarios are calculated as in Eq. (47). $E^{s,H}$ and $E^{s,EV}$ represent the total energy supplied to the household and to the EV respectively. Table 7 presents the streamlined LCA for the BESS and the rooftop solar system.

Table 6
Battery Energy Storage System (BESS) configuration for the Home Energy System (HES).

Battery Energy Storage System (BESS) for HES	
Parameter	Value
Cell type	Lithium Iron Phosphate (LFP)
Cell format	Cylindrical, 26650
Rated energy capacity (kWh)	5
Rated power (kW)	5
Initial State of Health (SOH)	100%
Battery model	R-int Equivalent Circuit Model (ECM) (based on [46,47])
Battery degradation model	Semi-empirical calendric and cyclic (based on [48,49])
Power electronics	AC/DC Converter (based on [50])
Ambient conditions	Constant temperature, no solar irradiation
Grid section efficiency	95% (assumed)

$$LEES = \frac{\varepsilon^{LEC,H} + \varepsilon^{LEC,EV} + \varepsilon^{gr} + (\varepsilon^{PV}) + [\varepsilon^{BESS}]}{E^{s,H} + E^{s,EV}} \quad (47)$$

In the baseline scenario H0, we consider that the household electric loads and the EV charging load are met entirely with power drawn from the grid. In this case, the energy system consists of one grid component and two load components — the household load and the EV. The

Table 7
Streamlined LCA for the Battery Energy Storage System (BESS) and Photovoltaic Solar (PV) solar system in the Home Energy System (HES) (based on [43,44]).

Home Energy System (HES) Streamlined LCA			
Component	Production ($kgCO_2eq$)	End-of-Life (EOL) ($kgCO_2eq$)	Source
BESS			
Cells	803.71	−58.41	[53,54]
Power Electronics	399.43	−47.26	[55–58]
Miscellaneous Electronics	90.56	−13.12	[55,58]
Sum	1293.70	−118.79	
Total (BESS)		**1174.91**	
Photovoltaic Solar System			
Panels	5500.00	37.00	[60–62]
Power Electronics	489.80	−47.26	[55–58]
Sum	5989.80	−10.26	
Total (PV system)		**5979.54**	

Table 8
Simulation results for the four Home Energy System (HES) scenarios.

Simulation results home energy system				
	Scenario			
Parameter	H0	H1	H2	H3
Application				
Energy consumed (H) (MWh)	87.38	87.38	87.38	87.38
Energy consumed (EV) (MWh)	37.40	37.40	37.40	37.40
Energy import (grid) (MWh)	124.8	95.9	74.01	81.54
Δ% (rel. to H0)		−23.18	−40.69	−34.65
PV energy (MWh)	–	90.19	90.19	90.19
Energy discharged (MWh)	–	–	21.84	14.69
Δ% (rel. to H2)		–	–	−32.75
Energy export (grid) (MWh)	–	61.27	34.8	43.7
Δ% (rel. to H1)	–	–	−43.25	−28.67
Cumulative emissions (tCO_2)	58.91	48.59	40.96	36.87
Δ% (rel. to H0)	–	−17.52	−30.47	−37.41
LEES ($kgCO_2eq/kWh$)	0.4758	0.3930	0.3319	0.2991
Δ% (rel. to H0)	–	−17.39	−30.24	−37.13
BESS				
Lifetime (y)	–	–	20	20
Round-Trip Efficiency (%)	–	–	82.43	81.87
Remaining Capacity (%)	–	–	73.22	71.33
$\overline{SOC}$ (%)	–	–	24.82	49.41
$\overline{DOC}$ (%)	–	–	22.62	20.94
Equivalent Full Cycles (EFCs)	–	–	4952.53	3329.29
Mean C-rate (ch) (1/h)	–	–	0.16	0.12
Mean C-rate (dch) (1/h)	–	–	0.14	0.11
$\overline{SOCI}$ (gCO_2eq/kWh)	–	–	0	0

EV is treated as a load component; consequently, only unidirectional charging is permitted. Fig. 9 also depicts the baseline scenario. As there are no storage components in this configuration, the LEC emissions of both loads are composed solely of the GEC emissions. Another emissions category in this configuration is the grid operation emissions for the grid section within the system boundaries. This configuration is simulated for 20 years, and all emissions categories are tracked. In the numerator of Eq. (47), the bracketed quantities are not applicable to H0. The salient numerical results for this scenario are listed in Table 8. Cumulative emissions for H0 amount to around 59 t Carbon Dioxide Equivalent (CO_2eq), accompanied by a LEES value of 0.4758 kg CO_2eq/kWh at the end of 20 years. Fig. 10E depicts the cumulative emissions of the energy system over the simulated period. In Fig. 10F, the evolution of the LEES value over the simulation period is depicted. The LEES value remains largely constant over the simulation period in this scenario. The primary assumption of constant grid carbon intensity over the 20-year period may be considered as the worst-case scenario. The grid carbon intensity is expected to reduce year-over-year with increasing renewable generation capacity. Fig. 10G depicts the breakdown of this value and the contributions of the three emissions categories.

In scenario H1, the configuration from H0 is augmented by adding a rooftop PV solar system (Fig. 9). The installed PV solar system has a peak power rating of 5 kW_p. A standard annual PV solar power generation profile based on measured data for Munich, Germany, is used to obtain the generated power at each simulation timestep [65,68]. The EMS strategy *SimpleDeficitCoverage* regulates the power flows in this scenario. The energy system now consists of a generation component – the rooftop solar installation – and the components from H0. The lifetime emissions for such a system are described in Section 2.2. The energy generation emissions for a PV solar system are zero. Consequently, the GENEC emissions for both loads are also zero. The LEC emissions for both loads are still solely comprised of the GEC emissions. In the numerator of Eq. (47), the quantities in the square brackets do not apply to H1. Table 8 summarizes the important results for this scenario. The cumulative emissions drop to over 48 t. The LEES value drops to 0.3930 kg CO_2eq/kWh. The drop in cumulative emissions and the LEES value corresponds to over 17% as compared to scenario H0. Fig. 10E depicts the cumulative emissions of the energy system over the simulation period. Fig. 10F illustrates the trend of the LEES value over the simulation period. The LEES value starts from a high value and crosses the value for scenario H0 during the seventh year of operation and maintains this downward trend till the end of the simulated period, essentially implying that the system breaks even from an emissions perspective at this point. Fig. 10G presents the breakdown of the LEES value at the end of 20 years. The power generated by the rooftop solar system displaces some of the grid energy, causing the GEC emissions to be lower. The additional emissions due to the rooftop PV solar system are offset by the drop in GEC emissions,

Scenario H2 builds upon H1 by adding a residential BESS, i.e., a storage component is introduced in this scenario. Table 6 lists the relevant battery parameters. The lifetime emissions for the BESS are described in Section 2.4. For this scenario, we continue using the EMS strategy *SimpleDeficitCoverage* to control the energy flows. As the BESS is never charged with energy from the grid, the SOCI remains zero. As a result, no operation phase emissions are associated with the BESS, and no DEC emissions are associated with the two load components. At the end of 20 years, the cumulative emissions add up to around 41 t CO_2eq. In this case, all terms in Eq. (47) are applicable, and the LEES value is 0.3319 kg CO_2eq/kWh. These values represent a drop of over 30% vis-a-vis H0. From Fig. 10E, it can be seen that the emissions start at a higher value as compared to H1 due to the additional production and EOL emissions of the BESS. After the second year of operation, the cumulative emissions are already lower than in H1. During the fifth year, the cumulative emissions fall below those in H0 and remain lower till the end of the simulated period. Fig. 10F depicts the evolution of the LEES value, and the same trend is also observed here. From Fig. 10G, it can be seen that the additional emissions due to the production of the BESS are more than offset by a more substantial reduction in the GEC emissions. During the simulation period, the BESS is subjected to over 4950 EFCs with a mean DOC of over 22%. The mean SOC during this period is around 25%, and the SOH reaches a value of around 73% (Figs. 10A, B, D). Fig. 10C depicts the total energy supplied to the load and the total energy discharged from the BESS.

Scenario H3 is physically identical to H2 but is run with the *RHOptimization* EMS strategy. Although not explicitly prohibited, the strategy never chooses to charge the BESS with grid energy. Consequently, the SOCI remains zero, as in H2. The operation emissions for the BESS and

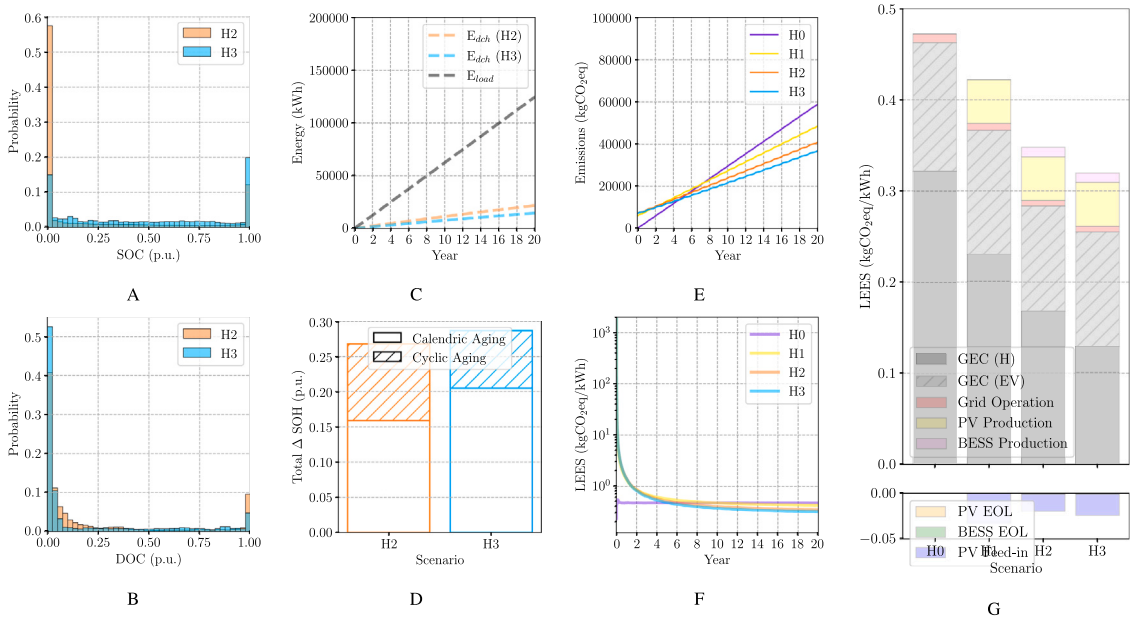

Fig. 10. A, B: Distributions of SOC and DOC values respectively in scenarios H2 and H3 over the simulated period. C: Depiction of the cumulative supplied energy for the four Home Energy System (HES) scenarios and energy discharged in scenarios H2 nd H3 over the simulated period. D: Change in the battery SOH over the simulated period and shares of calendric and cyclic aging in scenarios H2 and H3. E: Cumulative emissions for the four HES scenarios over the simulated period. F: Evolution of the Levelized Emissions of Energy Supply (LEES) value for the HES scenarios over the simulated period. G: Breakdown of LEES values for the HES scenarios into the constituent emissions categories at the end of the simulation period.

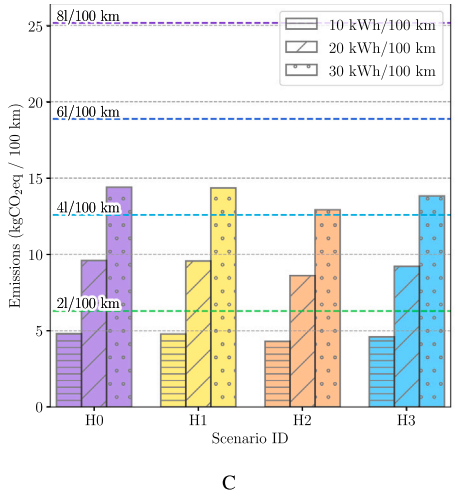

Fig. 11. Energy consumption emissions for EVs in the four HES configurations for the three energy economy levels considered relative to the four indicative fuel economy levels for internal combustion vehicles.

the DEC emissions for both loads are also zero. At the end of 20 years, the cumulative emissions, in this case, add up to over 36 t, and these are associated with a LEES of 0.2991 kg CO_2eq/kW h. This represents a drop of over 37% vis-a-vis H0. From Fig. 10E, it can be seen that the emissions start at the same value as H2 but remain lower from the get-go, reaching the lowest value among all scenarios by the end of the simulation. The LEES trend depicted in Fig. 10F exhibits the same behavior, with H3 attaining the lowest LEES among all scenarios. 10G depicts a snapshot of the emissions category-wise breakdown of the LEES value at the end of the simulated period. The lower LEES can be attributed to the optimal scheduling of the BESS to discharge energy at times with the highest grid carbon intensity values. This effectively reduces the GEC emissions of the household while marginally increasing the GEC emissions for the EV. The net reduction, however, manages to offset the production and EOL emissions of the PV solar system and the BESS. Figs. B.1–B.3 in the appendix depict the evolution of some more parameters of interest. In this scenario, the BESS is subjected to around 3330 EFCs with a mean DOC of around 21%. The mean SOC during this period is over 49%, and the SOH reaches a value of just over 71% (Figs. 10A, B, D). Despite the lower number of EFCs and the lower mean DOC than in H2, the total degradation is greater in H3, with a larger proportion of calendric degradation. This is attributed to the higher mean SOC, which leads to dominant calendric degradation for this cell type. Fig. 10C depicts the total energy supplied to the load and the total energy discharged from the BESS.

Fig. 11 depicts the energy consumption emissions of the EV for three energy economy scenarios with each of the four scenarios per 100 km driven. The three EV energy economy scenarios considered here are — 10 kW h/100 km, 20 kW h/100 km, and 30 kW h/100 km. The CO_2 emissions for four reference fuel-economy values for vehicles with petrol engines are also indicated on the plot — 2 l/100 km, 4 l/100 km, 6 l/100 km, and 8 l/100 km [69,70]. These values also reflect the fuel's well-to-wheel emissions without considering other emissions associated with the distribution infrastructure. It can be seen that there is barely any difference in the values for scenarios H0 and H1. This can be explained by the fact that the installed power of the PV system is much lower than the peak charging power, and a substantial number of charging events occur after sunset. There is a reduction in the EV emissions for scenario H2, as this strategy discharges the BESS right after it is charged, which possibly overlaps more frequently with the EV charging events. The higher EV emissions in scenario H3 imply that the EMS strategy optimizes for both loads taken together and is unable to selectively supply the EV with low carbon PV solar energy

while reducing the combined footprint of both the loads. Significantly, this analysis indicates that the energy consumption emissions for a moderately efficient EV are much lower than those for a vehicle with a very efficient petrol engine (4 l/100 km).

4. Conclusion and outlook

This article introduces Energy System Network (ESN) — an open-source energy system simulation program written in Python. The supporting mathematical framework to enable a time-resolved, component-wise, bottom-up calculation of the various emissions categories is described comprehensively. Two case studies to demonstrate the usage of this program have also been presented. The first case study investigates a grid-connected BESS application — energy arbitrage. The second case study looks at a home energy system with an electric vehicle.

An unconventional energy arbitrage strategy to shift energy from periods of low grid carbon intensities to periods of high grid carbon intensities has been explored in addition to the conventional profit-driven variant. The emissions-reducing strategy attains a LEES value over 17% lower while sacrificing 26% of the profits as compared to the conventional energy arbitrage. This shows that while emissions-driven energy arbitrage differs from the profit-driven variant, it is not entirely contrary to it. These results also Future market design studies to develop compensation mechanisms and revenue streams to incentivize such energy arbitrage strategies monetarily, which could spark exciting developments in this area. The Home Energy System (HES) simulations show that solely drawing power from the grid entails a lower carbon footprint in the first few years of operation while resulting in the highest emissions over the 20-year period. Integrating a rooftop PV solar system alone leads to a LEES reduction of over 17% and lower emissions from the seventh year of operation. Integrating a rooftop PV solar system coupled with a BESS home storage results in a LEES reduction of over 30% compared to the base case and lower operation emissions from just before the sixth year of operation. An emissions-reducing optimal EMS strategy can unlock a further LEES reduction of 7% points vis-á-vis the base scenario, which results in lower emissions from the fifth year of operation. For the EV in the base scenario, the energy consumption emissions for a moderate energy economy of 20 kW h/100 km are slightly higher than the emissions attributable to an internal combustion vehicle with an unrealistically low fuel economy of 3 L/100 km. All other scenarios fare better than the base scenario, if not comparably. This indicates that for the energy consumed for mobility, the present grid energy mix already fares better than fossil fuel combustion. This analysis does not consider the carbon footprint of the production and EOL phases of the vehicles,

The results of the two presented case studies must be interpreted with their limitations in mind. For both studies, perfect foresight has been assumed for all forward-looking time series data. Real-world forward-looking time series data will inevitably suffer from forecasting and prediction errors. The grid carbon intensity time series profile is assumed to remain static over the entire duration of the simulation. As historical data reveals an enduring downward trend in the grid carbon intensity, our assumption represents a worst-case scenario. Modeling an evolving grid carbon intensity profile is not a trivial matter of scaling down the entire profile by an arbitrary amount, as future values for grid carbon intensities are highly dependent on the shares and scheduling of participating generation technologies and the prevalent market and policy mechanisms.

The code base of this program is open-source, enabling the scientific community to use it for their own studies and possibly even contribute to further development of features. Complementary features from other energy system tools could also be coupled with ESN to enhance the scope of studies possible. For instance, the grid carbon intensity calculation functionality available in the tool elmada is a valuable feature [35]. The focus of this article has been limited to single energy systems primarily centered around a single energy form — electricity. Future functionality to support interconnected networks comprising multi-vector energy systems can enable studies on multi-modal energy systems and sector coupling. Other future functionalities, including sizing calculations for energy system components and demand-side management, will enhance the program's ability to estimate the carbon footprint of energy systems. An economic evaluation suite is also conceivable for integration with the program to complement the carbon footprint analysis.

CRediT authorship contribution statement

Anupam Parlikar: Conceptualization, Data curation, Formal analysis, Investigation, Methodology, Software, Visualization, Writing – original draft, Writing – review & editing. **Benedikt Tepe:** Data curation, Formal analysis, Investigation, Visualization, Writing – original draft, Writing – review & editing. **Marc Möller:** Software, Writing – review & editing. **Holger Hesse:** Formal analysis, Funding acquisition, Supervision, Visualization, Writing – review & editing. **Andreas Jossen:** Funding acquisition, Resources, Supervision, Writing – review & editing.

Declaration of competing interest

The authors declare that they have no known competing financial interests or personal relationships that could have appeared to influence the work reported in this paper.

Data availability

Data will be made available on request.

Declaration of Generative AI and AI-assisted technologies in the writing process

During the preparation of this article, the authors used Grammarly in order to check the syntax and grammar of the text. After using these services, the authors reviewed and edited the content as needed; and take full responsibility for the content in the publication.

Acknowledgments

This research is funded by the German Federal Ministry of Education and Research (BMBF) via the research project greenBattNutzung (grant number 03XP0302D). The project is overseen by Project Management Juelich (PtJ). The authors express their gratitude to Houman Heidarabadi for his assistance in facilitating the open-source code release.

Appendix A. Additional plots (grid-connected applications)

See Figs. A.1 and A.2.

Appendix B. Additional plots (HES)

See Figs. B.1–B.3.

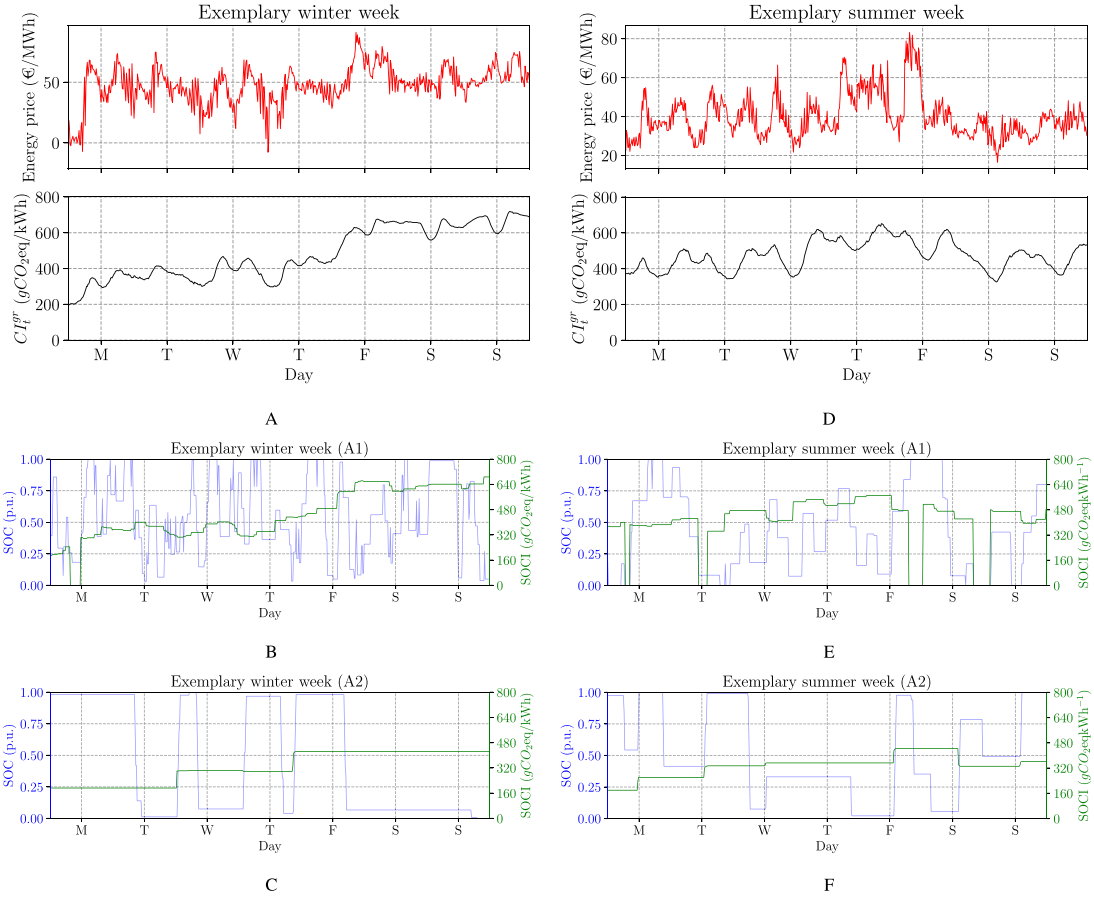

Fig. A.1. A, D: Energy prices and grid carbon intensity evolution with respect to time for an exemplary winter and summer week, respectively. B, C: State of Charge (SOC) and State of Carbon Intensity (SOCI) evolution with respect to time for an exemplary winter week for scenarios A1 and A2, respectively. E, F: State of Charge (SOC) and State of Carbon Intensity (SOCI) evolution with respect to time for an exemplary summer week for scenarios A1 and A2, respectively.

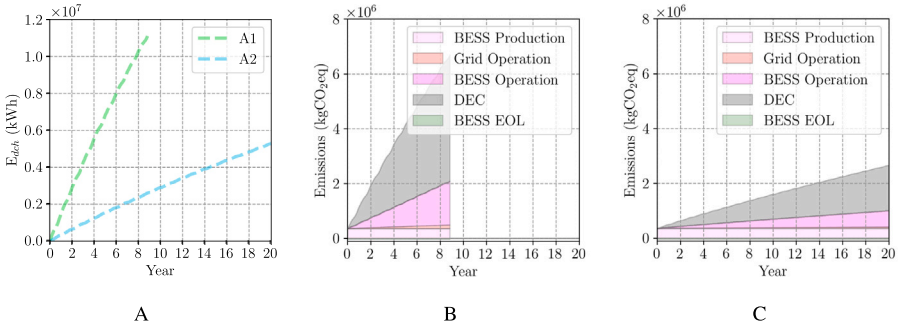

Fig. A.2. A: Energy discharged from the BESS in scenarios A1 and A2. B, C: Category-wise cumulative emissions in scenarios A1 and A2, respectively.

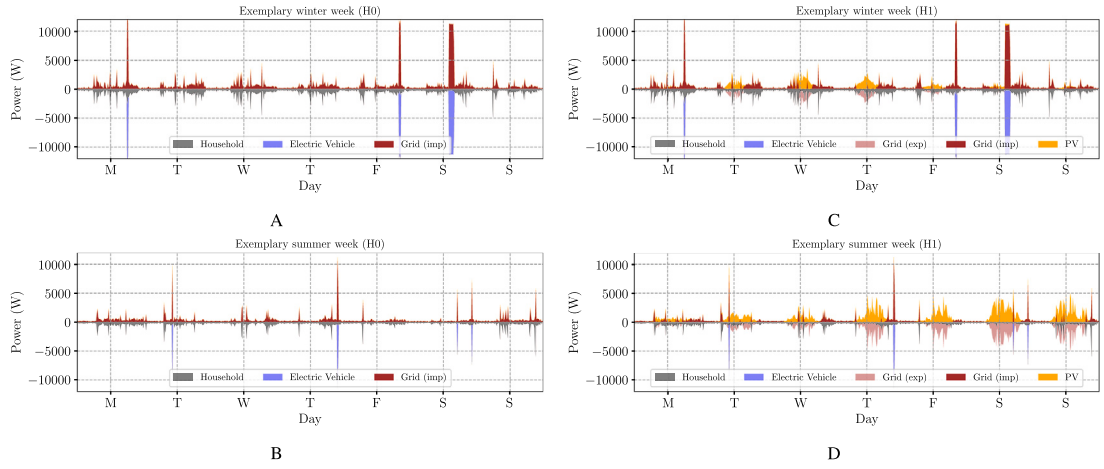

Fig. B.1. A, C: Power flows among energy system components for an exemplary winter week for scenarios H0 and H1, respectively. B, D: Power flows among energy system components for an exemplary summer week for scenarios H0 and H1, respectively.

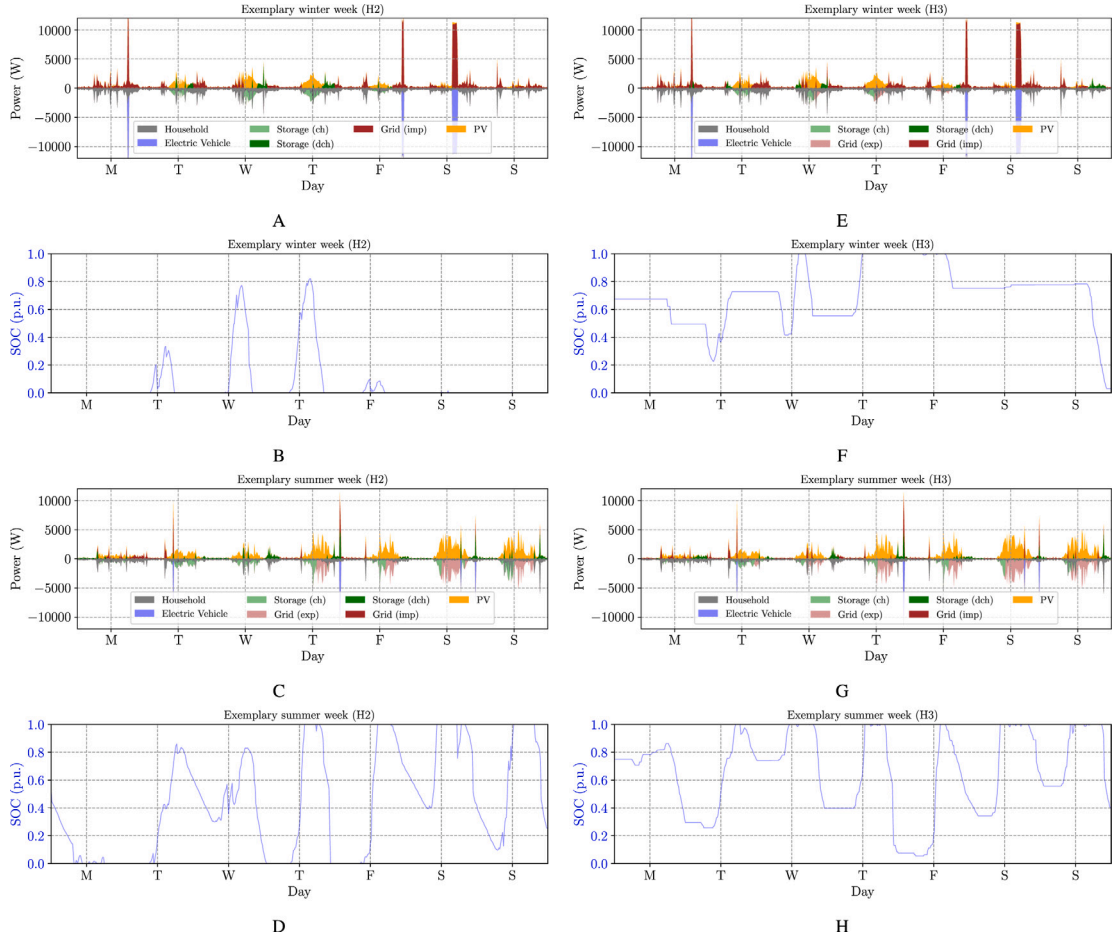

Fig. B.2. A, E: Power flows among energy system components for an exemplary winter week for scenarios H2 and H3, respectively. B, F: State of Charge (SOC) evolution with respect to time for the exemplary winter week for scenarios H2 and H3, respectively. C, G: Power flows among energy system components for an exemplary summer week for scenarios H2 and H3, respectively. D, H: State of Charge (SOC) evolution with respect to time for the exemplary summer week for scenarios H2 and H3, respectively.

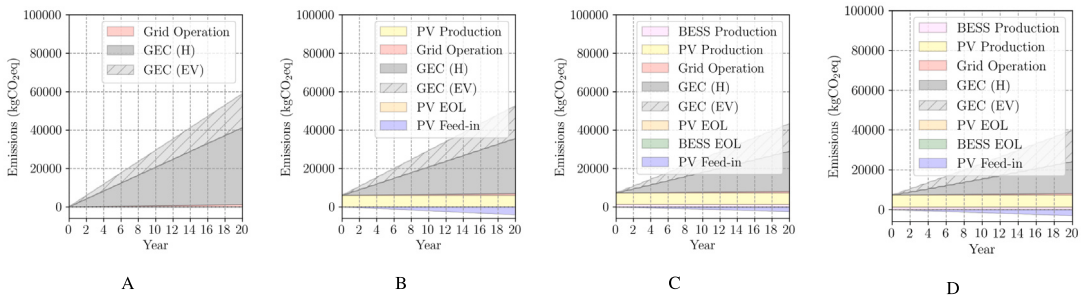

Fig. B.3. A, B, C, D: Category-wise cumulative emissions in scenarios H0, H1, H2, H3 respectively.

References

[1] International Renewable Energy Agency. Renewable capacity statistics 2023. Abu Dhabi: International Renewable Energy Agency; 2023, URL https://mc-cd8320d4-36a1-40ac-83cc-3389-cdn-endpoint.azureedge.net/-/media/Files/IRENA/Agency/Publication/2023/Mar/IRENA_RE_Capacity_Statistics_2023.pdf?rev=d2949151ee6a4625b65c82881403c2a7.

[2] DeCarolis J, Daly H, Dodds P, Keppo I, Li F, McDowall W, et al. Formalizing best practice for energy system optimization modelling. Appl Energy 2017;194:184–98.

[3] Hesse H, Schimpe M, Kucevic D, Jossen A. Lithium-ion battery storage for the grid—A review of stationary battery storage system design tailored for applications in modern power grids. Energies 2017;10(12):2107.

[4] Kebede AA, Coosemans T, Messagie M, Jemal T, Behabtu HA, van Mierlo J, et al. Techno-economic analysis of lithium-ion and lead-acid batteries in stationary energy storage application. J Energy Storage 2021;40:102748.

[5] International Energy Agency. Global EV outlook 2023. Paris: International Energy Agency; 2023, URL https://www.iea.org/reports/global-ev-outlook-2023.

[6] Figgener J, Hecht C, Haberschusz D, Bors J, Spreuer KG, Kairies K-P, et al. The development of battery storage systems in Germany: A market review (status 2023). 2023, URL http://arxiv.org/pdf/2203.06762v3.

[7] Gutsch M, Leker J. Global warming potential of lithium-ion battery energy storage systems: A review. J Energy Storage 2022;52:105030.

[8] Brown T, Hörsch J, Schlachtberger D. PyPSA: Python for power system analysis. J Open Res Softw 2018;6(1):4.

[9] Lund H, Thellufsen JZ, Østergaard PA, Sorknæs P, Skov IR, Mathiesen BV. EnergyPLAN – advanced analysis of smart energy systems. Smart Energy 2021;1:100007.

[10] Lund H, Thellufsen JZ. EnergyPLAN - advanced energy systems analysis computer model: documentation version 16.2. Aalborg: Zenodo, Sustainable Energy Planning Research Group, Aalborg University, Denmark; 2022, http://dx.doi.org/10.5281/zenodo.6602938, URL https://www.energyplan.eu/training/documentation/.

[11] Pfenninger S, Pickering B. Calliope: A multi-scale energy systems modelling framework. J Open Source Softw 2018;3(29):825.

[12] Calliope contributors listed in AUTHORS. Calliope: A multi-scale energy systems modelling framework: Documentation. 2024, URL https://calliope.readthedocs.io/en/stable/index.html.

[13] Eshraghi H, de Queiroz AR, DeCarolis JF. US energy-related greenhouse gas emissions in the absence of federal climate policy. Environ Sci Technol 2018;52(17):9595–604.

[14] TEMOA Developer Team. Temoa project documentation. 2024, URL https://temoacloud.com/temoaproject/Documentation.html.

[15] Dorfner J. Urbs: A linear optimisation model for distributed energy systems: Documentation. 2014, URL https://urbs.readthedocs.io/en/latest/index.html.

[16] Dorfner J. Open source modelling and optimisation of energy infrastructure at urban scale [Ph.D. thesis], Munich, Germany: Fakultät für Elektrotechnik und Informationstechnik, Technical University of Munich; 2016, URL https://mediatum.ub.tum.de/1285570.

[17] Krien U, Schönfeldt P, Launer J, Hilpert S, Kaldemeyer C, Pleßmann G. Oemof.solph—A model generator for linear and mixed-integer linear optimisation of energy systems. Softw Impacts 2020;6:100028.

[18] Hilpert S, Kaldemeyer C, Krien U, Günther S, Wingenbach C, Plessmann G. The open energy modelling framework (oemof) - a new approach to facilitate open science in energy system modelling. Energy Strategy Rev 2018;22:16–25.

[19] Welder L, Ryberg D, Kotzur L, Grube T, Robinius M, Stolten D. Spatio-temporal optimization of a future energy system for power-to-hydrogen applications in Germany. Energy 2018;158:1130–49.

[20] FINE Developer Team. FINE - a framework for integrated energy system assessment: Documentation. 2023, URL https://vsa-fine.readthedocs.io/en/latest/index.html.

[21] US Department of Energy. GridLAB-D: A unique tool to design the smart grid. 2023, URL https://www.gridlabd.org/index.stm.

[22] Schneider KP, Fuller J, Tuffner F, Chen Y. Modern grid strategy: Enhanced gridlab-d capabilities: Final report. 2009, https://www.pnnl.gov/main/publications/external/technical_reports/PNNL-18864.pdf.

[23] Bahramara S, Moghaddam MP, Haghifam MR. Optimal planning of hybrid renewable energy systems using HOMER: A review. Renew Sustain Energy Rev 2016;62:609–20.

[24] UL Solutions. HOMER software. 2023, URL https://www.homerenergy.com/index.html.

[25] UL Solutions. HOMER pro 3.15: Documentation. 2023, URL https://www.homerenergy.com/products/pro/docs/3.15/how_homer_calculates_emissions.html.

[26] Freeman J. Recent and planned improvements to the system advisor model (SAM). Albuquerque, New Mexico, USA: NREL; 2019, URL https://www.nrel.gov/docs/fy22osti/74214.pdf.

[27] Blair N, DiOrio N, Freeman J, Gilman P, Janzou S, Neises T, et al. System advisor model (sam) general description (version 2017.9.5). 2018, https://www.nrel.gov/docs/fy18osti/70414.pdf.

[28] Electric Power Research Institute. DER VET user guide. EPRI; 2022, URL https://storagewiki.epri.com/index.php/DER_VET_User_Guide.

[29] Langiu M. COMANDO documentation. 2020, URL https://comando.readthedocs.io/en/latest/index.html.

[30] Langiu M, Shu DY, Baader FJ, Hering D, Bau U, Xhonneux A, et al. COMANDO: A next-generation open-source framework for energy systems optimization. Comput Chem Eng 2021;152:107366.

[31] Weniger J, Tjaden T, Orth N, Maier S. Performance simulation model for PV-battery systems (PerMod): Documentation. Version 2.1. Research group Solar Storage Systems, University of Applied Sciences Berlin; 2020, URL https://solar.htw-berlin.de/wp-content/uploads/HTW-PerMod-Dokumentation.pdf.

[32] Atabay D. An open-source model for optimal design and operation of industrial energy systems. Energy 2017;121:803–21.

[33] Atabay D. Ficus: A (mixed integer) linear optimisation model for local energy systems: Documentation. 2015, URL https://ficus.readthedocs.io/en/latest/.

[34] Fleschutz M, Bohlayer M, Braun M, Murphy MD. Demand response analysis framework (DRAF): An open-source multi-objective decision support tool for decarbonizing local multi-energy systems. Sustainability 2022;14(13):8025.

[35] Fleschutz M, Murphy M. Elmada: Dynamic electricity carbon emission factors and prices for europe. J Open Source Softw 2021;6(66):3625.

[36] Smith K, Gasper P. BLAST: Battery lifetime analysis and simulation tool suite. NREL; 2023, URL https://www.nrel.gov/transportation/blast.html.

[37] Möller M, Kucevic D, Collath N, Parlikar A, Dotzauer P, Tepe B, et al. SimSES: A holistic simulation framework for modeling and analyzing stationary energy storage systems. J Energy Storage 2022;49:103743.

[38] Hall LM, Buckley AR. A review of energy systems models in the UK: Prevalent usage and categorisation. Appl Energy 2016;169:607–28.

[39] Lopion P, Markewitz P, Robinius M, Stolten D. A review of current challenges and trends in energy systems modeling. Renew Sustain Energy Rev 2018;96:156–66.

[40] Pfenninger S, Hawkes A, Keirstead J. Energy systems modeling for twenty-first century energy challenges. Renew Sustain Energy Rev 2014;33:74–86.

[41] Prina MG, Manzolini G, Moser D, Nastasi B, Sparber W. Classification and challenges of bottom-up energy system models - a review. Renew Sustain Energy Rev 2020;129:109917.

[42] Pellow MA, Ambrose H, Mulvaney D, Betita R, Shaw S. Research gaps in environmental life cycle assessments of lithium ion batteries for grid-scale stationary energy storage systems: End-of-life options and other issues. Sustain Mater Technol 2020;23:e00120, URL http://www.sciencedirect.com/science/article/pii/S2214993718302318.

[43] Parlikar A, Schott M, Godse K, Kucevic D, Jossen A, Hesse H. High-power electric vehicle charging: Low-carbon grid integration pathways with stationary lithium-ion battery systems and renewable generation. Appl Energy 2023;333:120541.

[44] Parlikar A, Truong CN, Jossen A, Hesse H. The carbon footprint of island grids with lithium-ion battery systems: An analysis based on levelized emissions of energy supply. Renew Sustain Energy Rev 2021;149:111353.

[45] Fraunhofer Institute for Solar Energy Systems ISE. In: Burger B, editor. Electricity generation in Germany 2019. Freiburg, Germany: Fraunhofer Institute for Solar Energy Systems ISE; 2019, URL https://energy-charts.info/charts/power/chart.htm?l=en&c=DE&stacking=stacked_absolute_area&year=2019&interval=year.
[46] Schimpe M, von Kuepach ME, Naumann M, Hesse HC, Smith K, Jossen A. Comprehensive modeling of temperature-dependent degradation mechanisms in lithium iron phosphate batteries. J Electrochem Soc 2018;165(2):A181–93.
[47] Schimpe M, Becker N, Lahlou T, Hesse HC, Herzog H-G, Jossen A. Energy efficiency evaluation of grid connection scenarios for stationary battery energy storage systems. Energy Procedia 2018;155:77–101.
[48] Naumann M, Schimpe M, Keil P, Hesse HC, Jossen A. Analysis and modeling of calendar aging of a commercial LiFePO4/graphite cell. J Energy Storage 2018;17:153–69.
[49] Naumann M, Spingler FB, Jossen A. Analysis and modeling of cycle aging of a commercial LiFePO4/graphite cell. J Power Sources 2020;451:227666.
[50] Notton G, Lazarov V, Stoyanov L. Optimal sizing of a grid-connected PV system for various PV module technologies and inclinations, inverter efficiency characteristics and locations. Renew Energy 2010;35(2):541–54.
[51] Schimpe M, Naumann M, Truong N, Hesse HC, Santhanagopalan S, Saxon A, et al. Energy efficiency evaluation of a stationary lithium-ion battery container storage system via electro-thermal modeling and detailed component analysis. Appl Energy 2018;210:211–29.
[52] Parlikar A, Hesse H, Jossen A. Topology and efficiency analysis of utility-scale battery energy storage systems. In: Proceedings of the 13th international renewable energy storage conference 2019. IRES 2019, 2019, URL https://www.atlantis-press.com/proceedings/ires-19/125923324.
[53] Baumann M, Peters JF, Weil M, Grunwald A. CO 2 footprint and life-cycle costs of electrochemical energy storage for stationary grid applications. Energy Technol 2017;5(7):1071–83.
[54] Mohr M, Peters JF, Baumann M, Weil M. Toward a cell–chemistry specific life cycle assessment of lithium–ion battery recycling processes. J Ind Ecol 2020;24(6):1310–22.
[55] Wernet G, Bauer C, Steubing B, Reinhard J, Moreno-Ruiz E, Weidema B. The ecoinvent database version 3 (part i): Overview and methodology. Int J Life Cycle Assess 2016;21(9):1218–30.
[56] Hu A, Huang L, Lou S, Kuo C-H, Huang C-Y, Chian K-J, et al. Assessment of the carbon footprint, social benefit of carbon reduction, and energy payback time of a high-concentration photovoltaic system. Sustainability 2017;9(1):27.
[57] de Simón Martín M, Díez-Mediavilla M, Alonso-Tristán C. Real energy payback time and carbon footprint of a GCPVS. AIMS Energy 2017;5(1):77–95.
[58] Bulach W, Schüler D, Sellin G, Elwert T, Schmid D, Goldmann D, et al. Electric vehicle recycling 2020: Key component power electronics. Waste Manag Res : J Int Solid Wastes Public Clean Assoc ISWA 2018;36(4):311–20.
[59] Ylmén P, Peñaloza D, Mjörnell K. Life cycle assessment of an office building based on site-specific data. Energies 2019;12(13):2588.
[60] Reich NH, Alsema EA, van Sark W, Turkenburg WC, Sinke WC. Greenhouse gas emissions associated with photovoltaic electricity from crystalline silicon modules under various energy supply options. Prog Photovolt, Res Appl 2011;19(5):603–13.
[61] Latunussa CE, Ardente F, Blengini GA, Mancini L. Life cycle assessment of an innovative recycling process for crystalline silicon photovoltaic panels. Sol Energy Mater Sol Cells 2016;156:101–11.
[62] Reese MO, Glynn S, Kempe MD, McGott DL, Dabney MS, Barnes TM, et al. Increasing markets and decreasing package weight for high-specific-power photovoltaics. Nat Energy 2018;3(11):1002–12.
[63] Figgener J, Hecht C, Haberschusz D, Bors J, Spreuer KG, Kairies K-P, et al. The development of battery storage systems in Germany: A market review (status 2023). 2022, arXiv.
[64] Sun S, Crossland A, Chipperfield A, Wills R. An emissions arbitrage algorithm to improve the environmental performance of domestic PV-battery systems. Energies 2019;12(3):560.
[65] Kucevic D, Tepe B, Englberger S, Parlikar A, Mühlbauer M, Bohlen O, et al. Standard battery energy storage system profiles: Analysis of various applications for stationary energy storage systems using a holistic simulation framework. J Energy Storage 2020;28:101077.
[66] Tjaden T, Bergner J, Weniger J, Quaschning V. Repräsentative elektrische Lastprofile für Wohngebäude in Deutschland auf 1-sekündiger Datenbasis. Berlin, Germany: HTW Berlin - University of Applied Sciences; 2015, URL https://solar.htw-berlin.de/wp-content/uploads/HTW-Repraesentative-elektrische-Lastprofile-fuer-Wohngebaeude.pdf.
[67] Gaete-Morales C, Kramer H, Schill W-P, Zerrahn A. An open tool for creating battery-electric vehicle time series from empirical data, emobpy. Sci Data 2021;8(1):152.
[68] Zeh A, Witzmann R. Operational strategies for battery storage systems in low-voltage distribution grids to limit the feed-in power of roof-mounted solar power systems. Energy Procedia 2014;46:114–23.
[69] The ERM International Group Limited. Bp target neutral: Global online travel calculator: Method for calculating greenhouse gas emissions. 2021, https://www.bp.com/bptargetneutralnavapp/consumer/bpTN_Online%20Travel%20GHG%20Emissions%20Calculator_Updated%20Methodology%20Statement_01July2021.961acd71.pdf.
[70] Prussi M, Yugo M, De Prada L, Padella M, Edwards R. JEC well-to-wheels report v5: Anticipation and foresight, technical guidance. In: KJ-NA-30284-EN-N (online). Luxembourg (Luxembourg): Publications Office of the European Union; 2020.